
Evaluation of Algorithms for ECG Derived Respiration in the Context of Heart Rate Variability Studies



AALBORG UNIVERSITY
DENMARK

Lasse Sohrt-Petersen

Group 989

Master Thesis

Biomedical Engineering and Informatics

Aalborg University

Department of Health Science and Technology

Fredrik Bajersvej 7
9220 Aalborg Øst
Denmark

Title:

Evaluation of Algorithms for ECG Derived Respiration in the Context of Heart Rate Variability Studies.

Project Period:

Autumn 2013

Project Group:

Group 989

Participants:

Lasse Sohrt-Petersen

Supervisor:

John Hansen

Co-supervisor:

Johannes Jan Struijk

Copies: 4

Pages: 77

Appendices: 5

Finished: January 13th, 2014

The heart rate is modulated by the autonomic nervous system. Heart rate variability is an expression of the amount of variation in heart rate. A normal healthy autonomic nervous system, will yield a continuous varying heart rate, hence analysis of heart rate variability is a simple, noninvasive method for the evaluation of the autonomic nervous system. A major component of heart rate variability is respiratory sinus arrhythmia, which is respiration induced variation in heart rate. Therefore respiratory information is needed in the analysis of heart rate variability. Respiratory information can be obtained using designated devices, but it can also be derived from the electrocardiogram.

Several different methods for deriving respiratory information from the electrocardiogram have been published. In this thesis a selection of these methods were implemented and evaluated. On three healthy male subjects, a five minute electrocardiographic signal was recorded simultaneously with a respiratory air flow signal as a reference. Using each method respiratory information was derived from the electrocardiographic signal. The duration of each breath was identified in the surrogate signal and the reference signal. The correlation between the series of respiratory durations of the reference and the derived signal was analysed.

For one of the methods for deriving respiratory information from the electrocardiogram, it was not possible to derive a feasible respiratory signal. The rest of the methods all yielded signals that significantly correlated with the reference signal ($p < 0.001$, Pearson).

In conclusion the correlation between the majority of the methods for deriving respiratory information from the the correlation with the reference signal was significant. This indicates, that further studies in the use of electrocardiography derived respiration in the context of heart rate variability studies are justified.

Preface

This thesis has been prepared by Lasse Sohrt-Petersen in partially fulfilling the 4th semester project of the master of Biomedical Engineering and Informatics at the Department of Health Science and Technology at Aalborg University.

References in the thesis are stated according to the Vancouver-method, where the boxed number e.g. [18] refers to the 18th article in the list of bibliography. Citations prior to a full stop only refers to the last sentence. However, if the citations follow directly after a full stop it refers to the paragraph or section. Figures or tables that are not originally created in context to this project are annotated with the respective references to the source.

This thesis is organised as follows:

The initiating problem is presented in the Introduction. Part I of the thesis consists of the analysis of the initiating problem, a synthesis of this analysis and finally the Problem Statement.

Part II includes the problem solution. The requirements of the solution are formulated based on the Problem Statement. Then the design and implementation of the solution are described. Finally the results are presented.

Part III consists of a summary of the thesis. Here the results and the general procedures of the thesis are discussed and concluded upon. The thesis is accompanied by a number of appendices.

This report was prepared by:

Lasse Sohrt-Petersen

Contents

1	Introduction	6
I Problem Analysis		8
2	Overview of the Problem Analysis	9
3	The Conducting System of the Heart	10
4	The ECG Signal	13
4.1	Placement of Electrodes and ECG Leads	13
4.2	Appearance of the ECG signal	15
4.2.1	Cardiac Electrical Vector	16
4.2.2	Vectorcardiography	17
5	Respiratory-Induced Modulations of the ECG	19
6	ECG Derived Respiration	22
6.1	Literature Review of EDR Methods	22
6.2	Categorisation of the EDR Methods	25
6.2.1	Multiple Lead Methods Based on Variations in Angle of Mean Electrical Axis	25
6.2.2	Single Lead Methods Based on R-wave Amplitude or QRS Area	25
6.2.3	Methods based on heart rate	26
6.2.4	Methods Based Discrete Wavelet Transform and Bandpass Filtering	26
6.2.5	VCG Methods Based on Variations in Angle of Mean Electrical Axis	27
6.2.6	Combinative Methods	27
7	Problem Statement	28
7.1	Synthesis	28
7.2	Problem Statement:	29
II Problem Solution		30
8	Solution Strategy	31
9	Requirements	32
9.1	Solution Description	32
9.2	Specification of Requirements	32
10	Preprocessing	34

10.1	Filtering the ECG Signal	34
10.2	QRS Detection	36
10.2.1	QRS Detection - Stage 1	37
10.2.2	QRS Detection - Stage 2	38
11	EDR Algorithms	40
11.1	Multiple Lead Methods Based on Variations in Angle of Mean Electrical Axis	40
11.1.1	EDR1: Multi Lead Method based on Variations in Angle of Mean Electrical Axis	40
11.2	Single Lead Methods Based on R-wave Amplitude or QRS Area	42
11.2.1	EDR2A & EDR2B: R Wave Amplitude with Respect to Baseline	42
11.2.2	EDR3A & EDR3B: R Wave Amplitude with Respect to S Wave	42
11.2.3	EDR4A & EDR4B: QRS Area	42
11.3	Methods Based Wavelet Transform or Bandpass Filtering	43
11.3.1	EDR5: Wavelet Transform	43
12	Evaluation	45
12.1	Reference Signal	45
12.2	Respiratory Period Estimation	45
12.3	Performance Measures	46
12.3.1	Mean Square Error	46
12.3.2	Correlation Coefficient	46
12.3.3	Scatter Plots	47
13	Results	48
III	Summary	53
14	Discussion	54
15	Conclusion	56
	Bibliography	57
IV	Appendix	61
A	Data Collection Protocol	62
B	Pilot Study	66
C	Synthesis of the VCG	71
D	Respiration	73
E	Characteristics of QRS Detection Filters	76

Chapter 1

Introduction

Respiration and heartbeat are physiological functions critical for life. They are both modulated by fluctuations of the autonomic nervous system (ANS) and hence, they both carry information which can be used to investigate the autonomic control of the cardio-respiratory system. [15, 37]

Although the heart is able to beat independently of any nervous or hormonal influences, the spontaneous rhythm of the heart, called intrinsic automaticity, can be modulated by the ANS [33].

Over the last three decades studies have shown a significant relationship between the ANS and cardiovascular mortality, including sudden cardiac death [41, 45].

Various different methods are presently available to assess the status of the autonomic modulation of the heart [45]. Among these methods, analysis of heart rate variability (HRV) has emerged as a simple, noninvasive method to evaluate the sympatho-vagal balance [24, 45].

HRV expresses the amount of variations of both RR intervals and instantaneous heart rate. Generally a normal heart and a healthy ANS will yield a continuous variation of the sinus cycle, thus reflecting a balanced sympatho-vagal state and a normal HRV. A heart, that have suffered from myocardial necrosis will result in sympatho-vagal imbalance, which will be reflected by a diminished HRV [45, 46].

A major component of HRV is respiratory sinus arrhythmia (RSA). RSA is the naturally occurring beat-to-beat fluctuation in heart rate that occurs during a respiratory cycle [27]. Therefore it appears to be important to determine at least the average respiratory rate as a complementary information to heart rate in HRV analysis. The magnitude of RSA depends on respiratory rate. Hence, especially under non-laboratory conditions, the magnitude of RSA cannot be used as a simple index of vagal control. The respiratory rate is necessary for the correct interpretation of the vagally mediated RSA and high frequency component of HRV. [15].

The respiratory signal can be recorded with techniques like spirometry, pneumography, or plethysmography. These techniques require the use of cumbersome devices

that may interfere with natural breathing, and which are unmanageable in certain applications such as ambulatory monitoring, stress testing, and sleep studies. [7]

Another approach is to control respiration, by asking the subject to breath with a specific pace, thus overruling the ANS by cortical inputs [27]. The key question is now, how does controlled breathing affect RSA? It has been observed, that respiratory rate variability (RRV), the respiratory analogy to HRV, is present during spontaneous breathing [27]. Evidence has shown, that while RSA is the modulation of heart rate by respiration, spontaneous respiration is triggered by cardiac activity. Thus the relationship between respiration and heart rate is bi-directional. [27]

Nonetheless, the joint study of the respiratory and cardiac systems is of great interest and the use of methods for indirect extraction of respiratory information is particularly attractive to pursue. Hence, it is most convenient to use a physiological signal that does not alter respiration but is easily accessible and carries unambiguous information about respiration.

ECG is one such signal.

Initiating Problem:

How can spontaneous respiration be derived from the ECG?

Part I

Problem Analysis

Chapter 2

Overview of the Problem Analysis

In this part of the thesis, the initial problem will be analysed. The scope of the thesis is to derive a surrogate respiratory signal from the ECG. Before this can be done, some basic ideas and principles must be addressed.

In Chapter 3 the conducting system of the heart is introduced. The components of the conducting system are presented and the path of an electrical impulse is traced through the heart. It is this impulse, that forms the origin of the relevant biomedical signal, namely the ECG.

In Chapter 4 the ECG is presented. First an overview of the measurement of the ECG and the appearance of the ECG is given. Another electromagnetic cardiac signal, namely the vector cardiogram (VCG) is also introduced.

In order to extract respiratory information from the ECG, it is a prerequisite, that respiration induces modulations of the ECG. The respiratory modulations of the ECG are caused by a number of phenomena which are described in Chapter 5.

Chapter 6 introduces the concept of ECG derived respiration (EDR). The respiratory induced modulations of the ECG, are exploited to produce a respiratory surrogate. Various approaches have been presented in the literature. This chapter will provide a literature review of the approaches, as well as the signal preprocessing needed for their proper performance. Finally, the different approaches are categorised into groups of similar basic principle.

In Chapter 7, the problem analysis is synthesised and the problem statement of this thesis is presented.

Chapter 3

The Conducting System of the Heart

In a normal heart beat, two types of cardiac muscle cells are activated. Contractile cells provide the powerful contractions that propel the blood, while the specialised muscle cells of the conducting system provide the coordination of the contractions. Due to this coordination, the contractile cells pump blood in the right direction at the right time [3].

Unlike skeletal muscle, the muscle cells of the cardiac conducting system contracts spontaneously. This property is called automaticity or autorhythmicity. The rate and degree of contraction is controlled by the autonomic nerve system, ANS.

The conducting system consist of the:

- Sinoatrial node (SA node).
- Atrioventricular node (AV node).
- Atrioventricular bunde (AV bundle).
- Bundlebranches.
- Purkinje fibres.

In addition, conducting cells are found in the internodal pathways, which distribute the contractile stimulus through the atrium from the SA node to the AV node. See Figure 3.1.

Below the path of an impulse is traced through the conducting system of the heart [3].

Each heart beat is initiated by an action potential generated by the SA node, also called the cardiac pacemaker. The SA node is embedded in the posterior wall of the right atrium. See 1 in Figure 3.2.

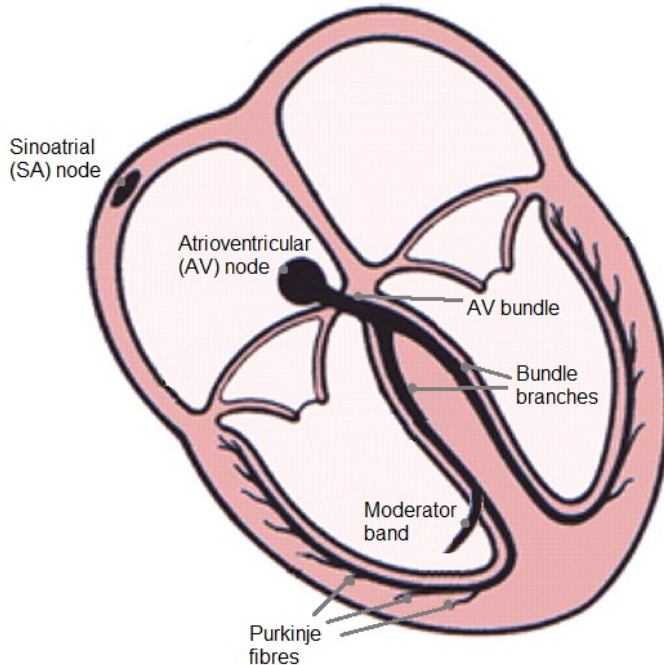


Figure 3.1: *Components of the conducting system [3, 37].*

The SA node and the AV node are connected by the internodal pathways in the atrial walls. The action potential travels through the internodal pathways in approximately 50 ms. Along the way the conducting cells stimulate the contracting cells of both atria. The action potential then travel across the atrial surface by cell-to-cell contact. This atrial stimulus is isolated from the ventricles by the cardiac skeleton. See **2** in Figure 3.2.

The larger AV node is placed within the floor of the right atrium. The cells of the AV node are smaller than the conducting cells of the atria. This causes the impulse to slow down as it leaves the internodal pathways and enter the AV node. In addition to this, the conduction between nodal cells is less efficient than that of the conducting cells. This delay of approximately 100 ms is important, as it allows the atria to fully contract before the ventricles do. See **3** in Figure 3.2.

After the delay, the impulse is carried through the interventricular septum, along the atrioventricular bundle and the bundle branches to the Purkinje fibres and the moderator band. This process takes approximately 25 ms. See **4** in Figure 3.2.

The moderator band stimulates the papillary muscles of the right ventricle. The papillary muscles prevent backward flow of ventricular blood into the atrial cavities by bracing the atrioventricular valves against prolapse. The Purkinje fibres distribute the impulse to the ventricular myocardium and ventricular contraction begins. Purkinje fibres conduct the impulse very rapidly. Within 50 ms, the impulse has reached all ventricular cardiac muscle cells. See **5** in Figure 3.2.

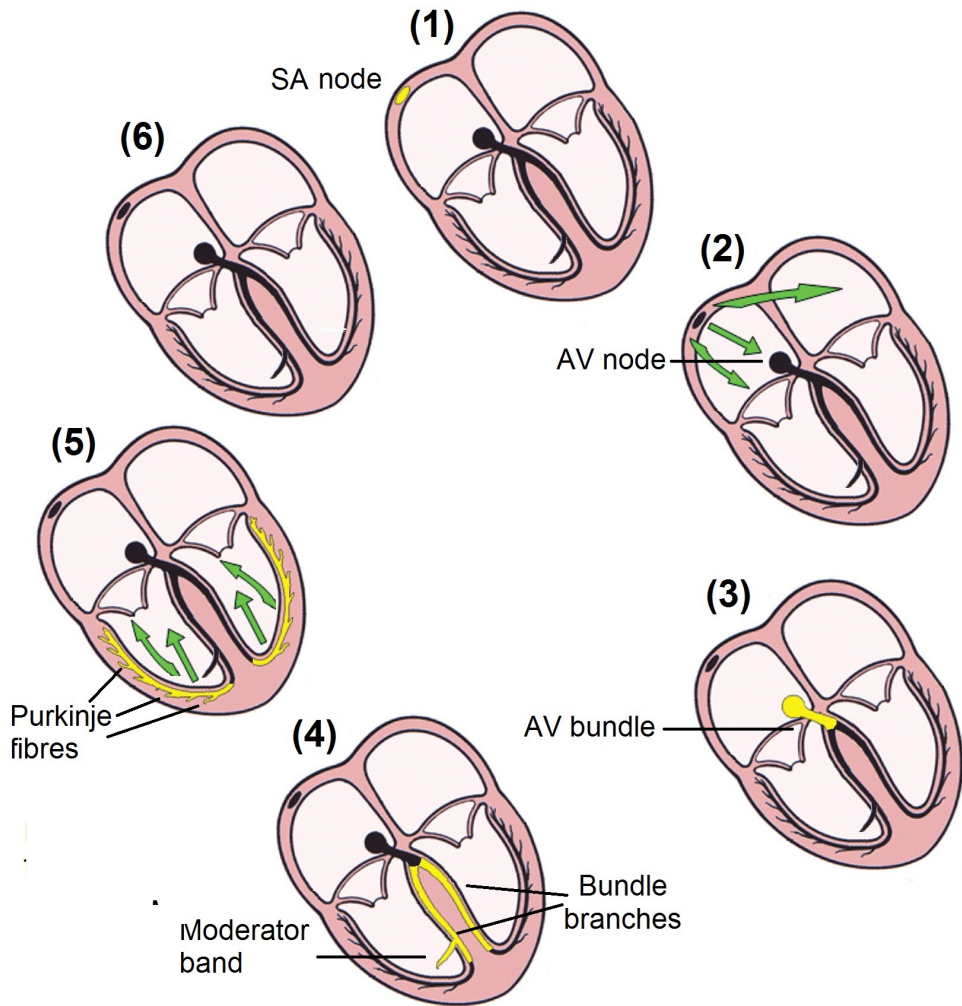


Figure 3.2: Impulse conduction through the heart. Yellow indicates activity in conduction components. Green indicates activity in contraction components. The figure is modified from [3, 37].

Chapter 4

The ECG Signal

The electrocardiogram (ECG) is a tool for evaluating the electrical conduction through the heart. ECG is typically measured via electrodes on the surface of the body. When the heart beats, a wave of depolarisation travels through the atria, reaches the AV node, travels down the interventricular septum to the apex of the heart, where it turns and spreads through the ventricular myocardium towards the base of the heart. [37, 48]

4.1 Placement of Electrodes and ECG Leads

A potential difference is measured between two points, so in order to measure a ECG signal, a minimum of two electrodes must be placed on the subject. The tracing of voltage between two electrodes is called a lead. Each lead produce a view of the heart from a different angle. Most ECG configurations include the three limb leads; lead I, lead II, lead III. The electrodes forming these leads are located on the limbs. One on each arm and one on the left leg. [43].

- **Lead I** is the voltage difference (V_I) between the left arm (LA) and the right arm (RA).
- **Lead II** is the voltage difference (V_{II}) between the left arm (LL) and the right arm (RA).
- **Lead III** is the voltage difference (V_{III}) between the left leg (LA) and the left arm (LA).

See Figure 4.1.

These leads form the basics of what is known as Einthoven's lead system. According to Kirchhoff's voltage law, the limb leads have the following relationship:

$$V_I + V_{III} = V_{II} \quad (4.1)$$

Conventionally, the lead vectors associated with Einthoven's lead system are found based on the assumption, that the heart, or more precisely the electrical center of the heart, is placed in the center of a equilateral triangle known as Einthoven's triangle. The limb electrodes can be placed on the shoulders and umbilicus of the

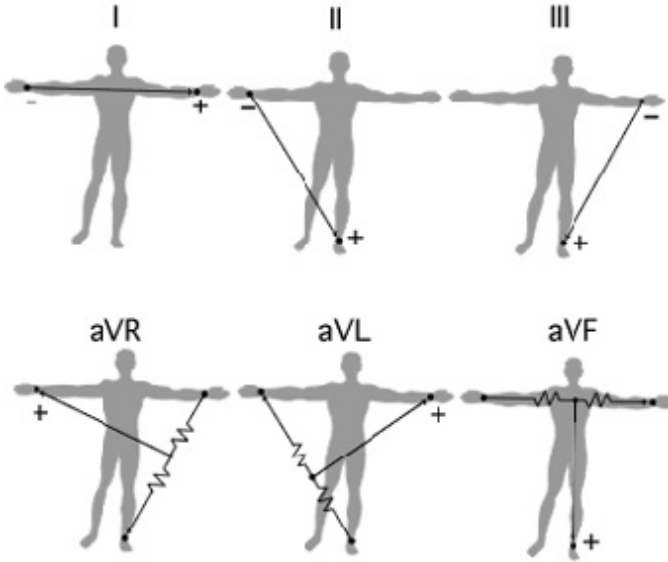


Figure 4.1: The figure illustrates the three limb leads and the three augmented limb leads. [39].

subject, thus producing the vertices of an equilateral triangle, having the heart located at its center. [36]

Two types of leads exist; unipolar and bipolar. The limb leads (Lead I, II, and III) are bipolar leads, as they have one positive and one negative pole. Unipolar leads also have two poles, however, the negative pole is a composite pole. The composite pole is called Wilson's central terminal (WCT). WCT is composed by connecting the limb electrodes RA, LA, and LL in a simple resistive network. This yields an average potential, which approximates the potential at infinity. [37]

$$WCT = \frac{1}{3}(RA + LA + LL) \quad (4.2)$$

Three additional limb leads called the augmented limb leads, utilises WCT to view the heart from different angles, without adding physical electrodes to the body. The three leads are called augmented vector right (aVR), augmented vector left (aVL), and augmented vector right (aVF). See Figure 4.1.

$$aV - R = RA - \frac{1}{2}(LA + LL) = \frac{3}{2}(RA - WCT) \quad (4.3)$$

$$aVL = LA - \frac{1}{2}(RA + LL) = \frac{3}{2}(LA - WCT) \quad (4.4)$$

$$aVF = LL - \frac{1}{2}(RA + LA) = \frac{3}{2}(LL - WCT) \quad (4.5)$$

Leads I, II, and III, and augmented limb leads; aVR , aVL , and aVF , form the basis of the hexaxial reference system, which is used to calculate the electrical axis of the heart in the frontal plane. [43] See Figure 4.2.

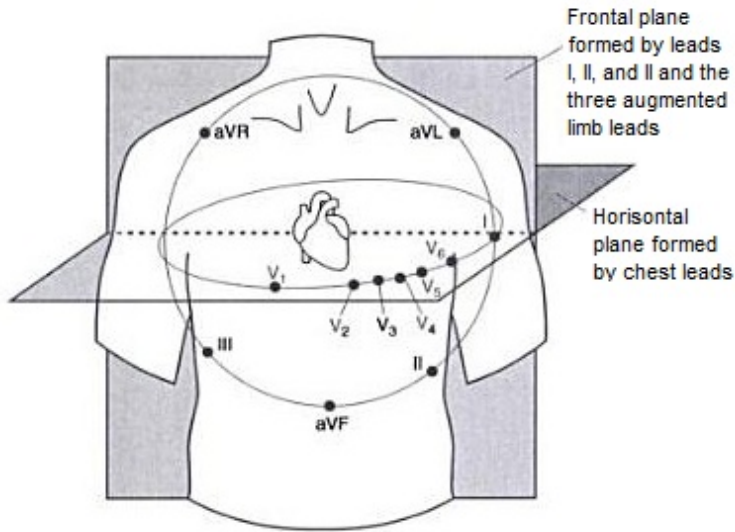


Figure 4.2: Placement of the precordial electrodes across the chest. The limb leads and augmented limb leads forms the electrical frontal plane of the heart. The precordial leads form the electrical horizontal plan of the heart. The figure is modified after [43].

For measuring the potentials of the hearts electrical axis in the horizontal plane, six electrodes can be placed directly across the chest. See Figure 4.2. These six electrodes as positive references and WCT as negative reference, composes the leads known as the precordial leads (V_1, V_2, V_3, V_4, V_5 and V_6). Due to the proximity to the heart, the precordial leads do not need augmentation. [43]

The limb leads, the augmented limb leads and the precordial leads together form the 12 lead system. Which is the most commonly used clinical ECG-system [36].

4.2 Appearance of the ECG signal

A typical ECG tracing of a normal cardiac cycle contains a P wave, a QRS complex, and a T wave as seen on Figure 4.3. The small P wave indicates the depolarisation of the atria. Contraction of the atria begin about 25 ms after the start of the P wave. [37]

The P wave is followed by a delay mainly caused by the AV node. The QRS complex appears as the ventricles depolarise. The magnitude of the QRS complex is bigger than the P wave, because the ventricular myocardium is much bigger than that of the atria. Ventricular depolarisation happens quickly because of the rapid conduction of the action potential through the Purkinje fibers. The QRS complex is a complex signal, mainly because the depolarisation spreads through relatively the complex pathways. Ventricular contraction occurs shortly after the the R wave. [37]

The smaller T wave represents ventricular repolarisation. Atrial repolarisation is

concurrent with ventricular depolarisation and does not appear in the ECG signal, because it is masked by the QRS complex. After the T wave a smaller U wave is sometimes apparent. It is hypothesised to be caused by the repolarization of the papillary muscles of the interventricular septum. U waves normally have a low amplitude, and are most often completely absent. The baseline voltage of the ECG is known as the isoelectric line. Typically the isoelectric line is measured as the portion of the tracing from the end of the T wave to the beginning of the next P wave (in case of absent U wave). [37]

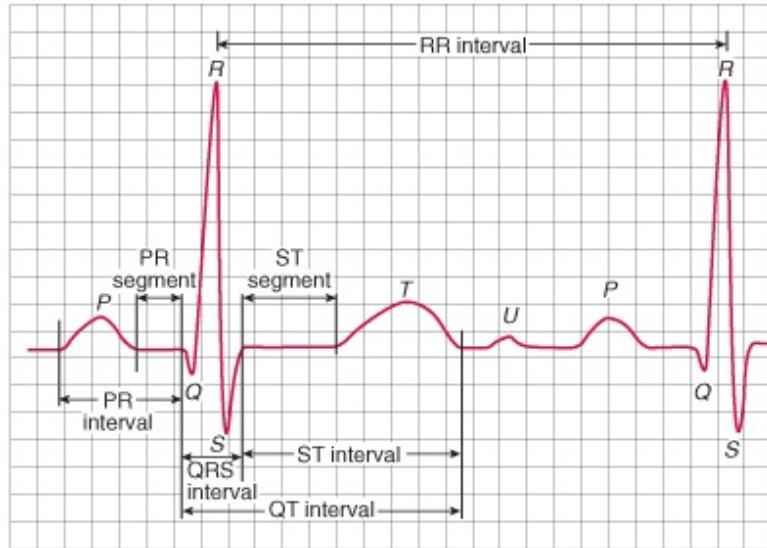


Figure 4.3: A sample of a normal ECG signal of a healthy subject. The most common segments and intervals and the various waves are indicated. The figure is modified from [37].

Assessment of the ECG signal include both the measurement of the magnitudes of the voltage changes and the determination of the durations and temporal relationships of the various components. The durations between waves are generally denoted segments or intervals. In general segments extend from the end of one wave to the start of another; whereas intervals always include at least one entire wave. Common intervals and segments are shown on Figure 4.3. For example:

The P-R interval is the duration from the start of atrial depolarisation to the start of the QRS complex, rather than to R. This is because that in abnormal ECGs the R peak can be difficult to determine. The Q-T interval indicates the duration of a single cycle of ventricular depolarisation and repolarisation. Usually measured from the end of the P-R interval, rather than from the bottom of the Q wave. [37]

4.2.1 Cardiac Electrical Vector

It can be assumed that the cardiac electrical generator of the heart is represented by a dipole (the cardiac electrical vector) located at the center of a sphere representing the torso, thereby at the center of an equilateral triangle (Einthoven's triangle). Thus the voltages measured by the limb leads are proportional to the projections of the cardiac electrical vector on the sides of the Einthoven's triangle. See Figure

4.4. The assumption is that the origin of the electric cardiac vector is in the center of the heart mass and remains there throughout the entire cardiac cycle and that the magnitude and direction of the vector changes throughout the cycle. [36]

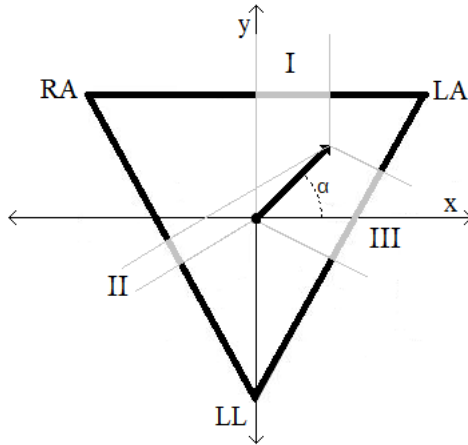


Figure 4.4: *Einthoven's triangle and the cardiac electrical vector.*

4.2.2 Vectorcardiography

Since the electric generator of the heart can be described by the an dipole, the cardiac electrical vector, it is natural to visually portray the electric generator of the heart in vector form. The measurement and interpretation of the cardiac electrical vector is called vectorcardiography. [36]

Basically the VCG is constructed by plotting the end point of the cardiac electrical vector in a three-dimensional space over time. The cardiac vector is constructed from three orthogonal leads, which are parallel to the axes of the three dimensional space. These coordinate axes can be either the body axes or the cardiac axes. See Figure 4.5

Plotting the cardiac electrical vector forms loops in the three dimensional space. The VCG consist of three distinct loops, namely the P-loop, the QRS-loop and the T-loop. Each loops respectively corresponds to the p-wave, QRS-complex and T-wave of the ECG.

When performing vectorcardiography, the main thing to consider is the distortions that is caused by the boundary and internal inhomogeneities of the body. Simply placing electrode pairs in the direction of a spatial line does not necessarily yield an equally oriented lead vector. To account for this corrected VCG lead systems have been developed to perform an orthonormal measurement of the cardiac electric vector. Here orthonormal implies that the three measured components of the cardiac electrical vector are orthogonal and parallel to the coordinate axes. Furthermore the measured components are detected with the same sensitivity (the measurements are normalised).

The most common corrected VCG lead system is the Frank lead system. The Frank lead system utilises seven electrodes in a resistive network to construct the three

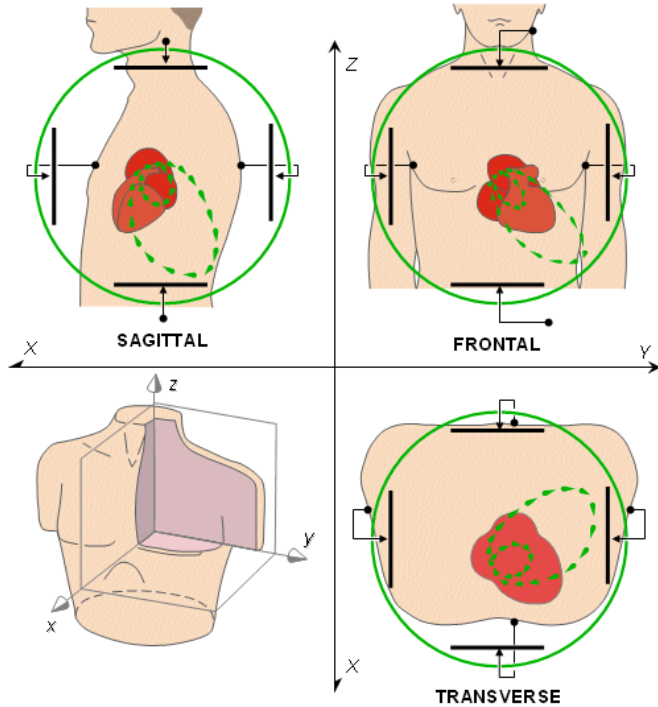


Figure 4.5: *The basic principle of VCG. Three orthogonal axes (here the body axes) are formed by three mutually orthogonal electrode pairs. The vector loop is projected on the principle planes. [36]*

orthogonal leads; X, Y, and Z, which is the components of the Back-to-front direction, right-to-left direction, and foot-to-head direction respectively [36].

Basically, the information content of the ECG and the VCG is the same. Roughly, an uncorrected VCG can be formed of the leads V_2 , V_6 , and $aV - F$ in the 12-lead ECG system. More elaborate techniques to synthesise the VCG from the ECG and vice versa have also been developed. In particular the inverse Dower transform synthesise the Frank lead VCG from the 12 lead ECG [12]. See Appendix C.

Chapter 5

Respiratory-Induced Modulations of the ECG

When the aim is to derive or estimate a surrogate respiratory signal from the information contained in the ECG signal, one have to observe the respiratory mechanisms that induce modulations of the ECG. It is known that the respiratory activity influences the measurements of ECG in various ways [7].

It has been shown experimentally, that the filling and emptying of the lungs during the respiratory cycle causes short term changes in thoracic impedance distribution [16]. The air that fills the lungs is a poor conductor compared to the different types of tissue, that make up the thorax. It is therefore feasible, that the inspiration of air increases the electrical impedance across the thorax. [17] A phenomenon which forms the basis for impedance plethysmography (See section 12.1), which is a method to measure respiratory activity [36].



Figure 5.1: *Respiratory induced modulation of R-peak amplitude. The upper trace is the ECG signal. The lower trace is a respiration signal measured by a pneumatic respiration transducer [17].*

The respiratory induced changes in thoracic impedance could lead one to conclude that inspiration would always decrease ECG amplitude and expiration would increase ECG amplitude. As can be seen in Figure 5.1. This is however not always the case.

ECGs recorded from the surface of the chest are also influenced by the relative motion of the electrodes with respect to heart. The expansion and contraction of the chest, which accompanies respiration, induces an apparent modulation in the direction of the mean cardiac electrical axis which affects beat morphology. [17, 29].

It has been experimentally shown that respiratory induced modulation of the electrical axis is caused mainly by the motion of the electrodes relative to the heart, while the thoracic impedance changes contribute to the electrical rotation as a second-order effect [7].

These physical influences of respiration result in amplitude modulations of the observed ECG [17]. Exemplified in Figure 5.1.

As described in the Introduction it is also well known that the ANS via RSA causes heart rate to increase during inspiration and decrease during expiration [27]. However, by bypassing autonomic control with a pacemaker it has been shown, that the mechanical action of respiration results in the same kind of frequency modulation in the ECG spectrum as does RSA [29].

Figure 5.2 shows an ECG trace as well as the corresponding heart rate and respiration signal. It can be seen, that the heart rate and respiratory signal fluctuate at a similar frequency.

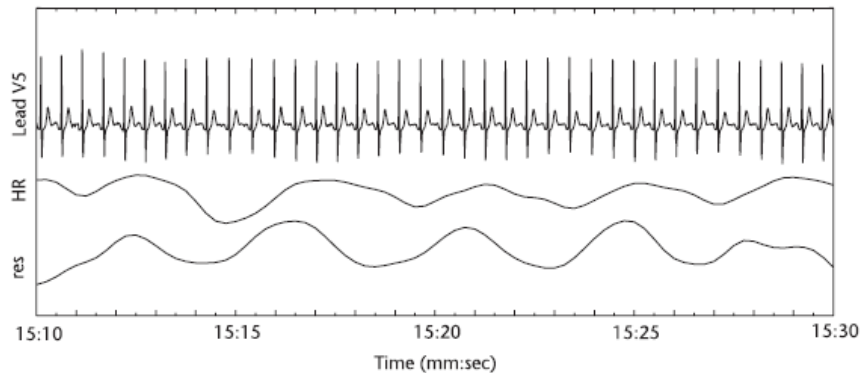


Figure 5.2: *Simultaneous ECG lead, heart rate, and respiration* [7].

Figure 5.3 shows the magnitude squared coherence, $|\Gamma(f)|^2$, between HR and respiration. The magnitude squared coherence is a measure of the correlation between two signals at a given frequency. It can be seen that signals are strongly correlated at around 0.3 Hz [7].

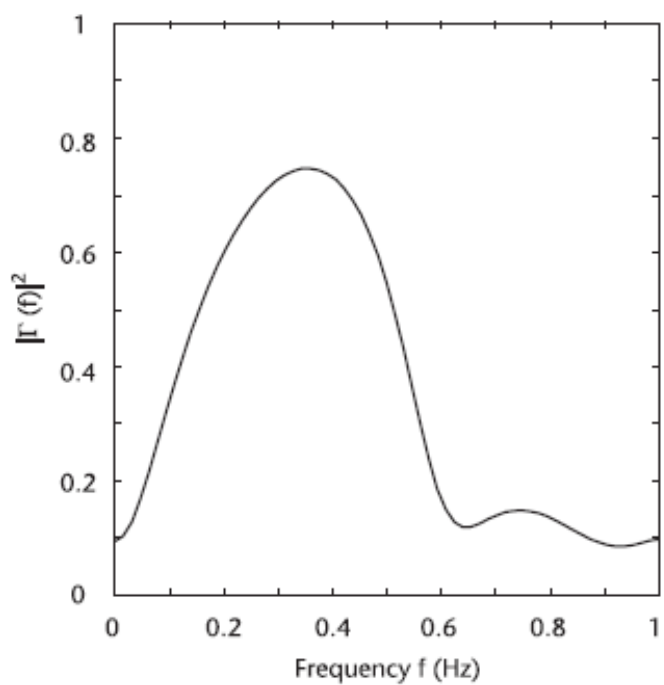


Figure 5.3: The Magnitude squared coherence, $|\Gamma(f)|^2$, between the heart rate and the respiratory signal corresponding to the signals of Figure 5.2 [7].

Chapter 6

ECG Derived Respiration

Several methods for extraction of a respiratory signal from the ECG, ECG-Derived Respiration (EDR), have been described in the literature. The EDR methods exploit the respiratory induced changes of the ECG to provide a surrogate respiratory signal, eg. a signal with varying amplitude corresponding to the different phases of respiration. These surrogate signals should enable the estimation of the respiratory rate and the temporal pattern of respiration. [28]

Some methods are based on respiration-induced variations in the beat-to-beat morphology, others extract respiratory information from variations in instantaneous heart rate. Also a combination of morphology and heart rate based methods have been proposed. A literature review of different EDR methods is provided below.

6.1 Literature Review of EDR Methods

The earliest attempt to derive a respiratory signal from the beat morphology of the ECG date back to 1974, when Wang et al. [47] proposed a technique for monitoring the respiratory rate, using the respiratory induced variation of the angle of mean electrical axis (AMEA) of the heart in relation to the body axes of the Frank-lead VCG. Although this is not strictly an ECG derived respiration, the ECG can be synthesised from the Frank-lead VCG and vice versa by means of the Dower transformation matrix [12], see Appendix C.

In 1985 Moody et al. [17] presented a multi ECG lead approach that utilised the AMEA. The AMEA was found as the arctangent of the ratio of the areas enclosed by the QRS complex of two orthogonal ECG leads. After subtracting the baseline, the areas were measured over a fixed windows in both ECG leads. The resulting EDR was visually compared to a recording of chest circumference and similarities between the two signals were reported.

Later Zhao et al. [23] quantified the correlation between the mean respiratory rate derived from the AMEA EDR and a reference signal. The overall correlation coefficient was found to be 0.9977 and a paired t test indicated that there was no difference between the mean respiratory rate derived from the EDR and the reference. In 1996 Caggiano and Reisman [8] investigated the effect of different QRS area windows. Two windows with variable window width performed better than a fixed width window, with correlation coefficients between the resulting EDR and a

6.1. LITERATURE REVIEW OF EDR METHODS

respiratory reference signal of 0.521 and 0.521 compared to 0.468. Measuring variations in AMEA have later been applied in sleep studies and HRV analysis [19, 22].

In 2003 Leanderson et al. [30] presented a different method of exploiting the respiratory induced variation of the AMEA. Instead of measuring the ratio of QRS areas in two ECG leads, estimation of the variation of AMEA was accomplished by spatiotemporal alignment of successive QRS-VCG loops with respect to a reference loop. The alignment method was originally developed to cancel out respiratory influence in the VCG signal, so that only morphologic variability of cardiac origin remained [44]. The method provides three EDR signals, namely the three angles constituting the rotation matrix that optimally describes the rotation needed to align the current QRS loop with the reference loop. Later Bailón et al. [35] extended the method by introducing an exponentially updated reference loop. The extended method proved to be more robust during stress testing [35].

Although the concept was previously mentioned [17, 29], in 1992 Khaled and Farges [34] was the first to exploit the simple principle of amplitude modulations of the single lead ECG. They found a respiratory surrogate by plotting the amplitude of the R wave with respect to baseline as a function of time. A qualitative comparison between the EDR signal and a impedance rheography signal lead to the conclusion, that the EDR signal was less sensitive to motion and cardiac artifacts.

In 1997 Felblinger et al. [31] used the same method to obtain a EDR signal, which was compared with the position of the diaphragm in inferior-superior direction measured during breath-holding MRI. The correlation coefficients between the two signals was in the range $r = 0.76$ to $r = 0.98$. In a similar manner Dobrev et al. 98 [11] used single lead QRS complex peak-to-peak amplitude (the sum of the absolut values of the R peak and the S peak) in apnea detection in infants. The EDR signal was visually compared to a impedance respirogram from a commercial cardiorespirograph. Again it was concluded that motion artefacts considerably affected the impedance respirogram, while the EDR signal remained adequate for apnea detection.

Mason and Tarassenko [38] compared the EDR signal from the R wave to baseline and the R wave to S wave methods. A breath detection algorithm was used to detect instances of respiratory onset in the two EDR signals. They found that the R wave to S wave method was superior to the R wave to baseline method, with a higher sensitivity (76.87% compared to 67.94%) and a higher positive predictivity (56% compared to 48.59%).

In 2007 O'Brien et al. [40] modified the R-wave to baseline method. Instead of interpolating the R-wave amplitudes at the occurrence of the corresponding R-wave in time, the amplitudes were interpolated evenly in time spacings corresponding to the average heart rate of the given series. In a comparison with a simultaneous inductance plethysmograph respiratory signal, the original and the modified methods yielded similar correlation coefficients ($r = 0.78$ and $r = 0.80$ respectively). The AMEA EDR of Behbani et al. [22] was also compared, showing worse correlation ($r = 0.63$). In 2007 O'Brien et al. [40] modified the R-wave to baseline method. Instead of interpolating the R-wave amplitudes at the occurrence of the corresponding R-wave in time, the amplitudes were interpolated evenly in time spacings corresponding to the average heart rate of the given series. In a comparison with a simultaneous inductance plethysmograph respiratory signal, the original and the modified methods yielded similar correlation coefficients ($r = 0.78$ and $r = 0.80$ respectively). The AMEA EDR of Behbani et al. [22] was also compared, showing worse correlation ($r = 0.63$).

In 2003 de Chazal et al. [9], in an attempt to identify classifiers for the automatic detection of obstructive sleep apnoea, produced an EDR signal from the area enclosed by the baseline corrected ECG signal in a window of $100ms$ after the R wave. In 2009 Arunachalam and Brown [6] used the ratio of the current R-wave amplitude and the running average of the previous R-wave amplitudes to estimate a real-time EDR signal.

Some EDR methods exploit the heart rate variability spectrum to derive respiratory information. The underlying idea is that the component of the HR in the HF band (above $0.15Hz$) generally can be explained by respiratory sinus arrhythmia. Most EDR algorithms based on HR information estimate the respiratory activity as the HF component in the HRV signal and, therefore, the HRV signal itself can be used as an EDR signal. To reduce HRV components unrelated to respiration, the HRV signal can be filtered. The signal of interest lies from 0.15 Hz to half the mean HR expressed in Hz, which is the highest meaningful frequency since the intrinsic sampling frequency of the HRV signal is given by the HR. [7]

The HRV signal is based on the series of beat occurrence times, obtained by detection of QRS complexes. A preprocessing step is needed in which QRS complexes are detected. Several definitions of signals for representing HRV have been suggested, for example, based on the interval tachogram, the interval function, the event series, or the heart timing signal. [7].

The presence of ectopic beats, as well as missed or falsely detected beats, results in fictitious frequency components in the HRV signal which must be avoided. Methods for deriving the HRV signal in the presence of ectopic beats based on the heart timing signal are available [20].

In 2002 Yi and Park [50] presented a method that did not rely on the detection of the QRS complex or any other salient point in the ECG. The principle was to isolate the components corresponding to the respiratory frequency band in the ECG signal. A discrete wavelet transform was applied to a lead II ECG signal. The EDR was found as the reconstruction of the detail signal of the 9th decomposition. The ECG was sampled at $200Hz$, which means, that the detail signal of the 9th decomposition correspond to $0.2 - 0.4Hz$. The instantaneous respiratory rates were extracted from the EDR and a respiratory airflow signal. The correlation between the two was reported as high ($r < 0.9$).

Later Boyle et al. [21] compared different wavelet decomposition methods, band-pass filtering methods, and HRV based methods. The mean respiratory rate was detected in the resulting EDR signals and compared to the mean respiratory rate detected in a reference signal. The methods that performed the best was filtering in the passband to $0.2 - 0.8Hz$ (mean error $< 20\%$) (no specific characteristics of the filter was mentioned) and combination of the HRV method and the $0.2 - 0.8Hz$ bandpass method (mean error $< 20\%$). The EDR methods with the worst performance yielded a mean error of around 50%.

Some methods derive respiration from the ECG by exploiting both beat morphology and HR. This process is based on the construction of a multichannel EDR signal. By crosscorrelating the power spectra of the EDR signals based on beat morphology and the heart rate based spectrum, the components unrelated to respiration can be reduced [30].

Another approach involves the use of adaptive filters which attenuates uncorrelated noise in two input signals, while common components are enhanced. E.g. the res-

piratory signal can be estimated by an adaptive filter applied to a series of RR intervals and the corresponding series of R wave amplitudes. [26]

6.2 Categorisation of the EDR Methods

This section will attempt to group the various published EDR methods into six distinct categories. This is done to provide a common denominator to groups of EDR methods based on similar principles. This will form a nomenclature that will be used through the remainder of this thesis.

The entries in each category are listed in chronological order according to publication date. Thus, the first publication of any given EDR principle is listed first, together with a short summary of the principle. Later methods are listed subsequently, with a short summary of the modification of the original principle.

6.2.1 Multiple Lead Methods Based on Variations in Angle of Mean Electrical Axis

Respiratory induced rotation of the mean electrical axis of the heart (AMEA) can be used to derive respiratory information from the ECG by tracking the angle between AMEA and a reference. The approach requires at least two approximately orthogonal ECG leads.

- *Moody 1985* [17] AMEA. The arctangent of the ratio of the QRS areas measured in a fixed window of two orthogonal, baseline subtracted ECG leads.
- *Zhao 1994* [23] AMEA. Fixed QRS area window. Leads: lead I and lead III.
- *Caggiano 1996* [8] AMEA. Three QRS area windows: 1) Window width independently fixed on each lead. 2) Window width independently variable on each lead. 3) Window width variable on one lead, the area of the other lead was measured in the same time interval.

6.2.2 Single Lead Methods Based on R-wave Amplitude or QRS Area

One of the simplest approaches is the interpolation of R-wave amplitudes or area of QRS complexes. This principle can be carried out on single lead ECG. The different methods vary mostly in the preprocessing of the ECG signal and in the choice of ECG-lead/electrode placement.

- *Khaled 1992* [34] R-wave amplitude with respect to baseline. Electrode placement: V2 and V3. Preprocessing: 8th order bandpass filter ($F_c = 2.5$ and $25Hz$).
- *Felblinger 1997* [31] R-wave amplitude with respect to baseline. Electrode placement: V2 and V3. Preprocessing: Bandpass filter ($F_c = 15$ and $21Hz$).
- *Dobrev 1998* [11] R-wave amplitude with respect to S-wave. Preprocessing: 1st order highpass filter ($F_c = 5Hz$), 2nd order lowpass ($F_c = 40Hz$).

- *Mason 2001* [38] R-wave amplitude both with respect to baseline and S-wave. The S-wave was defined as the minimum value in a window of 0.1 seconds after the R-wave. Preprocessing: Highpass filtering.
- *de Chazal 2003* [9] Area enclosed by baseline corrected ECG in the region $100ms$ following the the R-wave. Baseline correction: $200ms$ median filter to remove QRS complexes and P-wave, followed by $600ms$ median filter to remove T waves. The resulting signal was subtracted from the original ECG signal.
- *O'Brien 2007* [40] Two versions of R-wave amplitude with respect to baseline and one AMEA method. One where the R-wave amplitude is interpolated at the time instances of the R-wave and one were the R-wave amplitudes are interpolated evenly in time spacings corresponding to the average heart rate. Electrode placement: V5 for R-wave EDR and lead I and II for the AMEA EDR. Preproccesing: 20th order, high pass, linear phase, FIR filter, with Kaiser window ($\beta = 4$) ($F_c = 0.05Hz$).
- *Park 2008* [42] Area enclosed by the QRS complex in a $60ms$ window. Preprocessing: $50/60Hz$ notch filter. Baseline-wander was removed by subtracting the output of a $0.556ms$ median filter from the notch filtered ECG signal.
- *Arunachalam 2009* [6] Ratio of current R-wave amplitude and a running average of R-wave amplitudes. Preprocessing: 2nd order IIR notchfilter ($60Hz$ $Q = 14$) and 2nd order Butterworth lowpass filter ($F_c = 60Hz$ $Q = 14$). A baseline signal found using T-P knot interpolation is subtracted from the lowpass filtered ECG signal.

6.2.3 Methods based on heart rate

The heart rate varies as a function of respiration. This can be exploited to extract respiration.

- *Womack 1971* [49] Estimation of the time of occurence of breaths by filtering of the instantaous HR series.
- *Correra 2008* [25] Respiration represented simply as the RR-tachogram.

6.2.4 Methods Based Discrete Wavelet Transform and Band-pass Filtering

A simple and intuitive approach is to investigate the ECG signal content corresponding to the respiratory frequency band. The methods is applicable to single lead ECG recordings.

- *Yi 2002* [50] Discrete wavelet transform and reconstruction of the detail signal of the ninth decomposition, corresponding to the frequency band $0.2 - 0.4Hz$.
- *Boyle 2009* [21] Discrete wavelet transform and bandpass filtering. Biorthogonal spline wavelet decomposition: Reconstruction of detail signal of ninth decomposition (corresponding to frequency band: $0.3 - 0.6Hz$) and the sum of reconstruction of approximation signal of eighth decomposition and reconstruction of detail signal of ninth decomposition (corresponding to frequency band: $0.0 - 0.6Hz$). Bandpass filtering: $0.2 - 0.8Hz$ and $0.2 - 0.4Hz$.

6.2.5 VCG Methods Based on Variations in Angle of Mean Electrical Axis

The basic principle is to exploit a QRS-VCG loop alignment method to produce EDR signals corresponding to the rotation matrix needed to align QRS loops with a reference loop. The method have proved superior to methods based on heart rate and two lead AMEA variation [35].

- *Leanderson 2003* [30] QRC-VCG loop alignment with a predefined reference loop. The EDR signals results from the angels of the rotation matrix that optimally aligns the QRS loop with a reference loop.
- *Bailón 2003* [35] QRC-VCG loop alignment with a exponentially updated reference loop.

6.2.6 Combinative Methods

Methods deriving respiration from a combination of beat morphology and heart rate variability.

- *Varanini 1990* [26] Adaptive filtering of a R-wave EDR and a hear rate based EDR.
- *Orphanidou 2009* [14] Spectral fusion of EDR signals based on HRV and baseline wander.
- *Boyle 2009* [21] EDR signal formed by the average of EDR signals based on HRV and baseline wander.

Chapter 7

Problem Statement

7.1 Synthesis

HRV has been used extensively as a non-invasive tool to assess the influence of the ANS on the cardiovascular system [41]. A component of HRV is RSA, the instantaneous modulation of the heart rate caused by respiration. However, the relationship between respiration and heart rate is bidirectional [27]. Temporal variations in respiratory rate (RRV) is observed during spontaneous breathing. The RRV is caused by feedback mechanisms in much the same way that beat-to-beat heart rate fluctuations reflect different feedback mechanisms in cardiovascular control [15]. It has been demonstrated, that cardiac timing can be a significant determinant of RRV, altering breath-to-breath respiratory frequency. However, compared to HRV, RRV has received far less attention. [15, 27]

Attempts to uncouple these interrelationships in human experimental subjects have relied on pharmacological intervention, physical interventions such as altering body position, electrically stimulating the heart and the voluntary control of respiratory activity. [27]

With respect to controlled respiratory activity, the key question that remains unresolved is what does this do to RSA? Since controlled respiration removes the possible influence of cardiac activity on respiratory timing, we have disrupted the normal bidirectional system of which RSA is only a component outward manifestation.

This yields the need for respiratory measurement. It is possible to derive a surrogate respiratory signal from the ECG. Respiratory induced amplitude and frequency modulations of the ECG is caused by a combination of three different phenomena [28]:

- Respiratory induced modulation of the heart rate (RSA) leading to a frequency modulation of the ECG.
- The filling and emptying of air in the lungs leads to changes in the transthoracic impedance which lead to an amplitude modulation of the ECG.
- The mean electrical axis of the cardiac vector changes its direction during respiration, leading to both an amplitude modulation and a frequency modulation of the ECG.

7.2. PROBLEM STATEMENT:

The respiratory induced modulations of the ECG can be utilised to derive respiratory rates from the ECG, socalled ECG derived respiration (EDR). Several algorithms to do so have been published. Generally the algorithms can be divided into the following catagories [7]:

- EDR algorithms based on beat morphology, including:
 - Single Lead Methods Based on R-wave Amplitude or QRS Area
 - Multiple Lead Methods Based on Variations in Angle of Mean Electrical Axis
 - VCG Based Methods Based on Variations in Angle of Mean Electrical Axis
 - Methods Based Discrete Wavelet Transform and Bandpass Filtering
- EDR algorithms based on heart rate variabilty
- EDR algorithms based on a combination of beat morphology and heart rate variability

The different EDR methods all have their advantages and disadvantages. In general, EDR algorithms based on beat morphology are more accurate than EDR algorithms based on HR information. Some of the algorithms can estimate respiration from single lead ECG, while other require multiple leads. Some methods are a very accurate during sleep studies, while others prove robust during stress testing. [7] In conclusion; the choice of a particular EDR algorithm depends on the application.

This leads to following problem statement:

7.2 Problem Statement:

How can the performance of EDR methods in the estimation of spontaneous respiration in relation to the study of HRV be evaluated?

Part II

Problem Solution

Chapter 8

Solution Strategy

Part II of the thesis will be the problem solution, which is based on the problem stated in section 7.2. The problem solution will consist of five stages: "*Requirements*", "*Preprocessing*", "*Algorithms*", "*Evaluation*", and "*Results*".

The "*Requirements*"-stage consist of two sections, namely a generic description of the solution and a specification of the requirements of the solution. The requirements are formulated based on the problem statement.

The "*Preprocessing*"-, and "*Algorithms*"-stage include the selection and description of EDR algorithms that should meet the specified requirements and their required preprocessing. The selections is based on papers published in journals and books. The aim has been to apply several acknowledged and some newly published methods to investigate their performance in this application. The articles are collected from database searches mainly on: Pubmed and Google Scholar. [2, 5]

In the evaluation of data processing algorithms it is reasonable to choose a development environment in which algorithms are easily implemented and results are easily visualised. In this thesis, the implementation of the algorithms will be performed in MatLab. MatLab is a high-level language and interactive environment for numerical computation, visualisation, and programming [4].

The fourth and the fifth stage, *Evaluation* and *Results*, focuses on the evaluation of the algorithms. This includes a reference signal and performance measures. Finally the result of the evaluation is presented.

The problem solution will be aided by a of pilot study which can be found in Appendix B.

Two sets of ECG was used in this thesis. A database set from [13] was used in the implementation face, while a ECG was collected as a part of the thesis to be used in the evaluation of the algorithms. See Appendix A.

Chapter 9

Requirements

In this chapter the outlines of the solution to be produced through this project is described and the requirements to the solution are specified.

9.1 Solution Description

In chapter 7 it is stated that several methods for deriving a respiratory waveform from the ECG exist. The scope of this thesis is to evaluate and compare the performance of a number of these EDR algorithms. Generally the solution of this problem consist of two stages. First the EDR algorithms have to be identified and implemented. Secondly they have to be evaluated against some kind of 'gold standard' respiratory signal.

The first phase of the solution deals with the implementation and tuning of the EDR algorithms. This include the proper preprocessing of the ECG signal and the selection of ECG signals that is ought to meet the requirements stated below. The second stage, the evaluation stage, deals with the identification of a proper 'gold standard' reference signal and a number of performance measures. Finally the results are presented.

9.2 Specification of Requirements

The general objective of this thesis is to evaluate the performance of a number of EDR algorithms in the context of heart rate variability studies. The requirements to the solution is reflected by this. The EDR algorithms should be able to be perform adequately on ECG data that could have been recorded during a typical HRV study.

In response to a growing recognition of HRV as a indicator for the relationship between the autonomic nervous system and cardiac mortality, *The Board of the European Society of Cardiology and The North American Society of Pacing and Electrophysiology* established a *Task Force* with the responsibility of developing appropriate standards of nomenclature and methods of measurements in the research of HRV. The *Task Force* was established in 1994 and the were published in 1996 [41]. The recommendations of the standards will form the basis of the requirements to

the problem solution in this project.

Generally two kinds of HRV analysis recordings are recommended: Long term recordings and short term recordings. Short term recordings are carried out over 5 minutes and enables analysis of three distinguished spectral components: very low frequency ($VLF \leq 0.04Hz$), low frequency ($LF: 0.04 - 0.15Hz$), and high frequency ($HF: 0.15 - 0.4Hz$). Long term recordings are carried out over 24 hours and in addition it enables an ultra low frequency component ($ULF \leq 0.015Hz$). The ULF component reflects variability that can be assigned to circadian rythm, while the HF component is the one affected by respiration. Therefor the short term recordings will be the scope of this project. [41]

In order to localise the fiducial point in HRV analysis (commonly the QRS complex), it is satisfactory that the ECG recording equipment follow voluntary standards in terms of SNR, common mode rejection, bandwidth etc. A low sample rate may cause significant jitter in the localisation of the R wave, which alter the spectrum significantly. The sample rate should optimally be in the range $250 - 500Hz$. If lower, the R wave should be refined by means of interpolation. In this case, even sample rate of $100Hz$ could be sufficient. [41]

It is reported, that baseline and trend removal may effect the lower components in the spectrum. The frequency response of any filter should be checked in order to verify, that spectral components of interest are not significantly affected. Short term recordings containing ectopic beats, arrhytmic events and missing data should be not be used. How ever, such an discremination could introduce significant selection bias of the data. [41]

Under short term recordings, the physical activity, emotional circumstances and recording environment should be controlled and described. And the recording environment of individual subjects should be similar.

Finally, since the context of this thesis is the study of HRV, the EDR methods cannot be based on the respiratory variability of heart rate. That is, the EDR should be based on beat morphology alone.

System Requirements

In summary, the evaluation of the EDR algorithms should be performed on data that satisfies the following:

- The ECG should be recorded on equipment that satisfy voluntary standards.
- The sample rate should be $\geq 500Hz$ or the data should be interpolated to enhance the fiducial points in the ECG.
- The recordings of should be of 5 minute duration.
- The environment of the recording should be controlled, physiological stable and similar for all subjects.

And:

- The EDR algorithm cannot be based on hear rate information.

Chapter 10

Preprocessing

Before a respiratory signal can be derived from the ECG, an array of preprocessing procedures has to be performed on the signal. These procedures include filtering the ECG, and for some EDR algorithms, detection of the QRS complexes.

10.1 Filtering the ECG Signal

A crucial task in ECG signal processing is to denoise the signal of interest. In this thesis, the challenge is to filter out noise, while keeping variations in the ECG caused by respiration. [40] Several sources of noise that can corrupt the ECG signal exist. Common sources of noise include powerline interference, electrode contact noise, EMG noise, motion noise, and baseline wander. [48]

In order to better understand the wanted and unwanted components of the ECG signal, the composite amplitude, $R(t)$, of a detected R-wave can be modelled as [6]:

$$R(t) = r \cdot a(t) + n_P(t) + n_H(t) + n_G(t) + b(t) \quad (10.1)$$

where r is the true R-wave amplitude during the resting phase of a normal tidal breath, $a(t)$ is the amplitude modulation due to respiration, $n_P(t)$ is narrow band noise due to power line interference, $n_H(t)$ is other high frequency noise due to EMG etc., $n_G(t)$ is zero mean Gaussian white noise, and $b(t)$ is baseline offset and -wander.

The challenge now lies in finding an estimate of $a(t)$ in order to estimate the respiration.

The baseline wander, $b(t)$, is caused by respiration [14], but baseline drift can also be assigned to temperature variations [18]. Due to the relation between baseline wander and respiration, it is important not attenuate baseline wander too aggressively. The experimental ECG signal in this thesis was recorded with equipment containing internal analogue filtering, with a passband from 0.05Hz to 120Hz [1](See Appendix A). The high-pass cut off frequency of 0.05Hz was deemed sufficient to eliminate unwanted baseline wander, while preserving respiratory information. This assumes that the lowest breathing frequency is 3 breaths per minute (normal breathing frequency in resting adults is 12 to 20 breaths per minute (0.2Hz to 0.33Hz). See

appendix D).

Powerline interference, $n_P(t)$, can be caused by improper grounding of the ECG recording equipment or interference from surrounding electronic equipment. [18] An example of powerline interference is clearly visible in Figure 10.1, which shows a unfiltered ECG-sample and its corresponding single-sided amplitude spectrum. In the amplitude spectrum a spike is clearly visible at 50Hz.

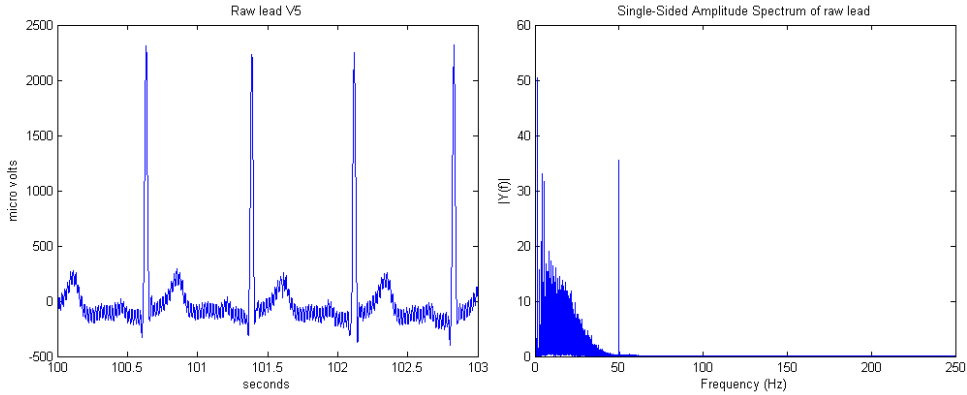


Figure 10.1: *A sample of ECG contaminated with 50Hz powerline interference and the corresponding single-sided power spectrum.*

The powerline interference is reduced using a 50Hz 2.–order IIR notch filter. After filtering in the forward direction, the filtered sequence is then reversed and run back through the filter using the `filtfilt`-function in MatLab. The result of this operation can be seen in Figure 10.2.

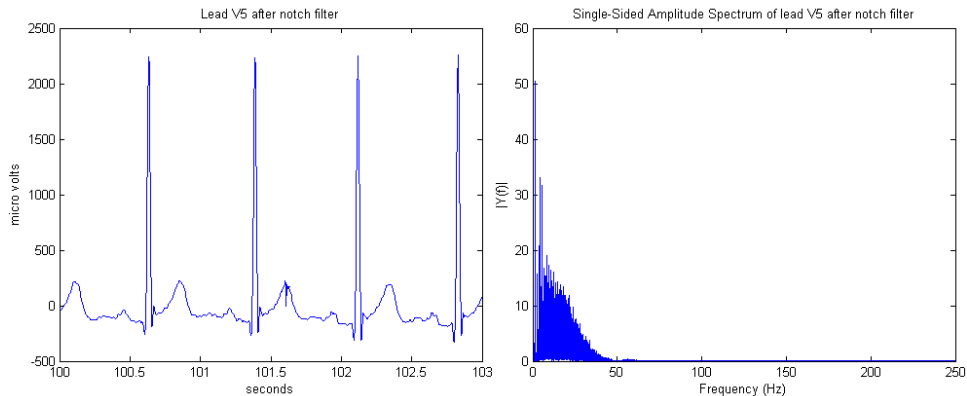


Figure 10.2: *A sample of ECG after notch filtering. The powerline interference has clearly been reduced and the single-sided power spectrum no longer show a spike at 50Hz. The reduction in powerline interference reveals a unwanted noisy event (just after 101.5 seconds)*

The remaining noise sources like EMG noise, $n_H(t)$, and zero mean Gaussian white noise, $n_G(t)$, is reduced with a 2.–order Butterworth low-pass filter with a cut-off frequency of 40 Hz. Like the notch filter, the low-pass filter is called with the `filtfilt`-function in MatLab. The combined result from the notch filter and the lowpass filter can be seen in Figure 10.3.

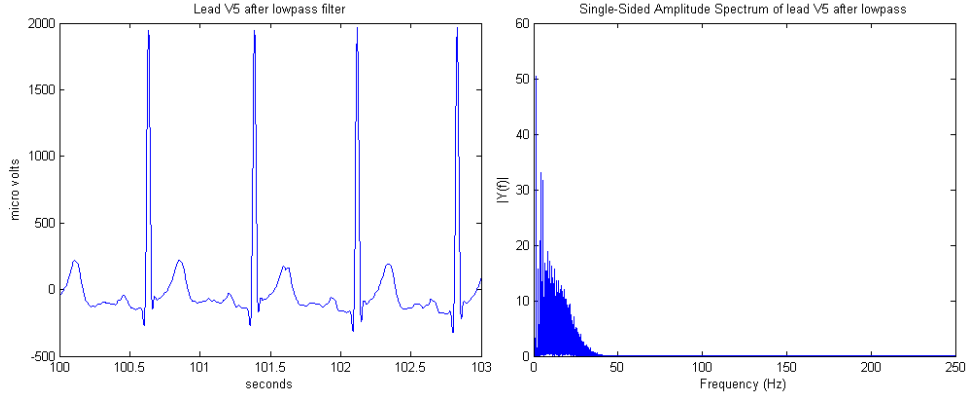


Figure 10.3: A sample of ECG after the combined notch filtering and lowpass filtering. The undetermined noise visible in Figure 10.2 has been reduced and the signal has been smoothed

10.2 QRS Detection

The majority of the EDR algorithms require the detection of a salient point in the ECG wave form, which can be found consistently on each beat. The feature most easily identified in the ECG is the QRS complex. Several QRS detectiong algorthms have been presented in the literature [18].

In this thesis, a modification of the Hamilton-Tompkins QRS detector will be implemented. The Hamilton-Tompkins QRS detector has shown a sensitivity of 99.69% and a positive predictivity of 99.77% [32], which makes it one of the most robust and proven QRS detector algorithms. The original QRS Hamilton-Tompkins detector consist of a two stages:

- Stage 1. A preprocessing stage including filtering, differentiating, squaring, and time averaging. The role of this stage is to enhance the enhance and isolate the QRS complex and is not to be confused with the preprocessing in Section 10.1. Stage 1 is summarised in Figure 10.4.
- Stage 2. A series of heuristic decisions rules which operates on the output of stage 1, in order to locate the QRS complexes in the original filtered ECG data.

See Figure 10.5 for the relationship bewteen the two stages of the QRS detector and the EDR preprocessing stage mentioned in Section 10.1.

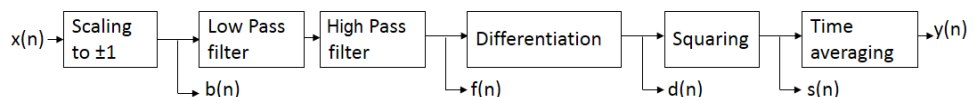


Figure 10.4: Filter stages of the QRS detector. $x(n)$ is the input signal, $b(n)$ is the signal normalised to ± 1 , $f(n)$ is the band pass filtered signal, $d(n)$ is the signal after differentiation, $s(n)$ is the signal after squaring, and $y(n)$ is the signal after time averaging.

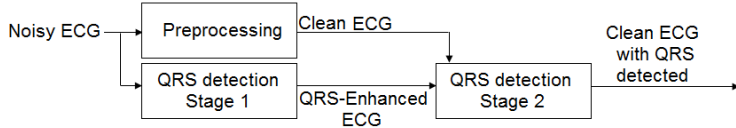


Figure 10.5: Overview of the combined filter and QRS detection stages. The noisy ECG is preprocessed two times separately. Firstly to reduce non respiratory information (Preprocessing) and secondly to enhance the location of QRS complexes (QRS detection Stage 1). The output of the QRS detection Stage 1 is a signal indicating the proximity of a QRS complex. In QRS detection Stage 2 this proximity information is used to perform a search back for peaks in the output of Preprocessing. This yields a clean ECG signal and the location of the QRS complexes of said signal.

10.2.1 QRS Detection - Stage 1

In the following, the steps of stage 1 of the QRS detection is explained. Figure 10.6 show the output of each step. (a) is the raw ECG signal. The original Hamilton-Tompkins QRS detector was developed for a sampling rate of 128Hz [32]. Many of the filterprocesses has been modified to accomdate a sampling rate of 500Hz . Each of the steps induce a delay.

Plot (b) show the output of the band pass filter. The band pass filtering is performed by cascading a low pass FIR filter and a high pass FIR filter to the raw ECG signal. The filter coefficients were generated in MatLab with the filter properties in Table 10.1. The combined filter impose a delay of 85 samples, which is corrected for later. The phase response of the filters is linear in the range of interest (between 5Hz and 30Hz). See the phase response and magnitude response of the filters can be seen in Appendix E.

Filter	Fstop(Hz)	Fpass(Hz)	Astop	Apass(Hz)	Order
High Pass	1	5	40	1	140
Low Pass	30	15	40	1	29

Table 10.1: Filter properties of the band pass filter.

Plot (c) show the output of the differentiation. The differentiation emphasises the higher frequency components of the ECG, such as the R wave. Differentiation is performed with a 4-point difference equation.

$$d(nT) = \frac{1}{8}(2f(nT) + f(nT - T) - f(nT - 3T) - 2f(nT - 4T)) \quad (10.2)$$

Where $d(nT)$ is the output of the filter at the n th sample. The difference equation imposes another two sample delay which is corrected for later.

Plot (d) show the effect of point squaring, $s(nT) = (d(nT))^2$. The baseline is aproaching zero, while the remaining spikes are at the proximity of the the R wave (bare in mind the uncorrected delay).

Plot e show the effect of time averaging over a 31 point window:

$$y(nT) = 131 \sum_{k=1}^{31} s(nT) \quad (10.3)$$

This step indicates the most likely location of the QRS complex. The step impose a 15 sample delay, which is corrected immediately.

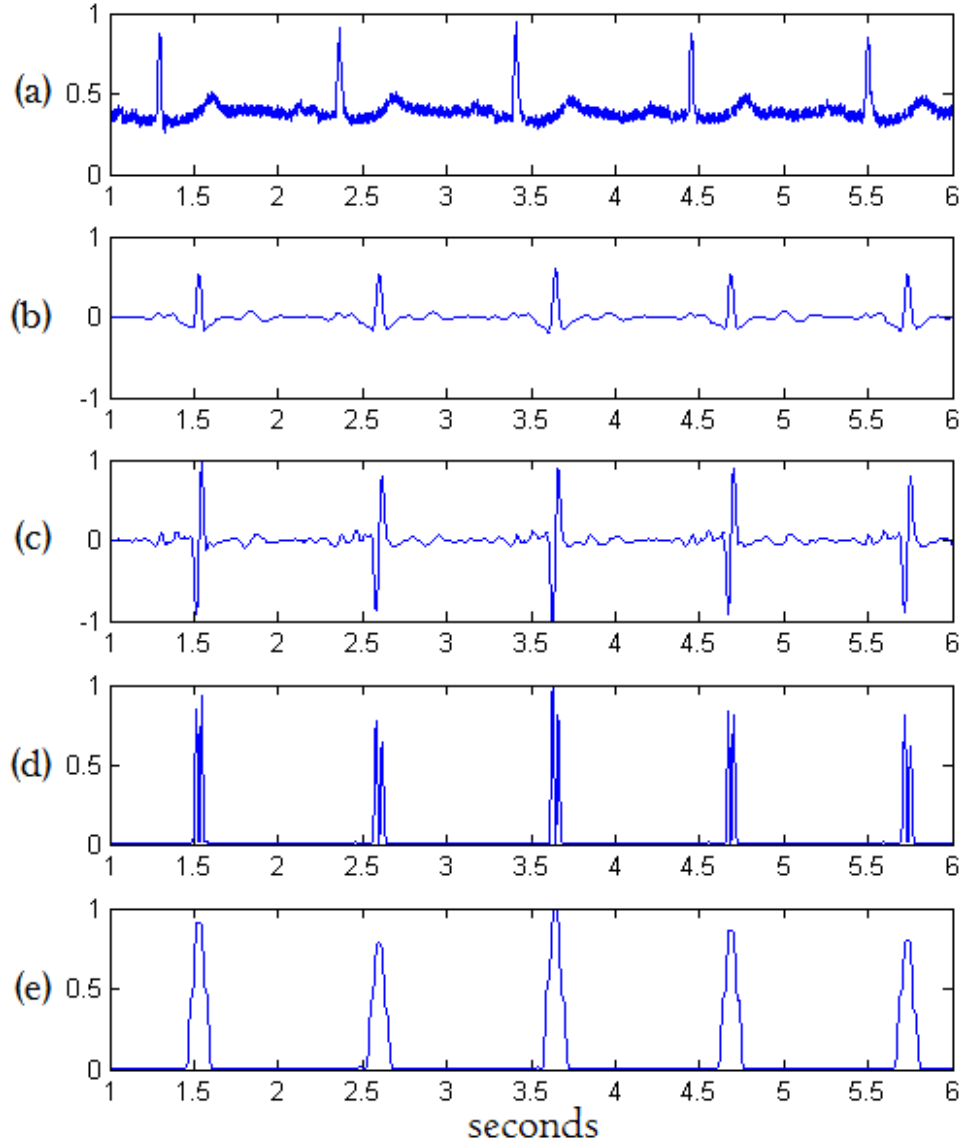


Figure 10.6: 5 seconds of ECG data at each step of stage 1 of the QRS detection.

10.2.2 QRS Detection - Stage 2

After correcting for the cumulative delay, the output of stage 1 of the QRS detector, is now used as one of the two inputs of stage 2. The other input is the ECG signal that has been filtered with regard to enhance respiratory information. In stage 2 of the QRS detector, the R wave is first identified by searching for a

maximum within a localised region of points whose amplitudes are greater than a threshold, set to be the median value of the last 5 R-waves. The search is performed in the clean ECG signal, and the region of the search is determined by the output of stage 1. The Q and S points are found as the minimum values on each side of the R point, within a region determined by the width of the approximately square waves, that is the output of stage 1.

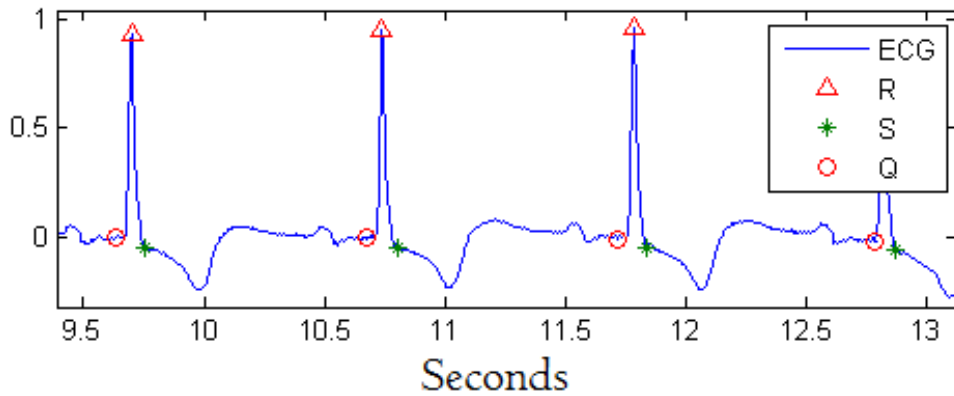


Figure 10.7: *ECG signal with annotated Q, R, and S points.*

In this thesis, the ECG sequences are of short duration (5 minutes). The performance of the QRS-detector is evaluated visually by plotting the ECG signal and the identified Q, R, and S points. See Figure 10.7. Any errors are manually corrected.

Chapter 11

EDR Algorithms

The following chapter will focus on the selection of EDR algorithms chosen for evaluation. All the EDR methods were presented in Chapter 6, but here the methods chosen for evaluation are elaborated. The motivation for the choice of each EDR method is elaborated in the section of that method. For the sake of convenience each EDR method is now given a name of type EDR1 through EDR4. Some of the EDR methods have the same basic principles and are only distinguished by minor differences. They are called EDR(*number*)A, EDR(*number*)B, etc.

- EDR1: Multi Lead Method based on Variations in Angle of Mean Electrical Axis.
- EDR2A: R Wave Amplitude with Respect to Baseline on Lead II.
- EDR2B: R Wave Amplitude with Respect to Baseline on Lead V4.
- EDR3A: R Wave Amplitude with Respect S Wave on Lead II.
- EDR3B: R Wave Amplitude with Respect S Wave on Lead V4.
- EDR4A: QRS Area on Lead II.
- EDR4B: QRS Area on Lead V4.
- EDR5: Methods Based on Discrete Wavelet Decomposition and Bandpass Filtering.

11.1 Multiple Lead Methods Based on Variations in Angle of Mean Electrical Axis

11.1.1 EDR1: Multi Lead Method based on Variations in Angle of Mean Electrical Axis

In this method, the projection of the mean electrical axis on the plane defined by two leads is considered. The variation in angle between reference lead and this projection is used as an estimate of the respiration [17]. The area of the i th QRS complex, occurring at time instant t_i , is computed over a time interval in each lead.

11.1. MULTIPLE LEAD METHODS BASED ON VARIATIONS IN ANGLE OF MEAN ELECTRICAL AXIS

The area is proportional to the projection of the mean electrical axis on that lead.

Consider the projection of the mean electrical axis on the plane jk , defined by orthogonal leads j and k , at time instant t_i , denoted as the vector $\bar{m}(t_i)$

$$\bar{m}(t_i) = \begin{bmatrix} \frac{1}{\delta_2 + \delta_1} \int_{t_i - \delta_1}^{t_i + \delta_2} \|m(t)\|_2 \cos(\theta_{jk}(t)) dt \\ \frac{1}{\delta_2 + \delta_1} \int_{t_i - \delta_1}^{t_i + \delta_2} \|m(t)\|_2 \sin(\theta_{jk}(t)) dt \end{bmatrix} = \frac{1}{\delta_2 + \delta_1} \begin{bmatrix} A_j(t_i) \\ A_k(t_i) \end{bmatrix} \quad (11.1)$$

where $m(t)$ is the instantaneous projection of the electrical axis on the jk -plane, $\theta_{jk}(t)$ is the angle between $m(t)$ and the reference lead j , $A_j(t_i)$ and $A_k(t_i)$ represents the QRS area in lead j and k respectively. The integration interval over which the mean is computed is defined by δ_1 and δ_2 . $\|\cdot\|_2$ denotes the Euclidean distance. The term $\|m(t)\|_2 \cos(\theta_{jk}(t))$ is representing the projection of $m(t)$ on lead j and $\|m(t)\|_2 \sin(\theta_{jk}(t))$ is the projection lead k . [7]

The angle of projection of the mean electrical axis on the jk -plane with respect to lead j is estimated as:

$$\theta_{jk}(t_i) = \arctan(A_k(t_i)/A_j(t_i)) \quad (11.2)$$

The fluctuations of this angle can now be used as an EDR signal. See Figure 11.1

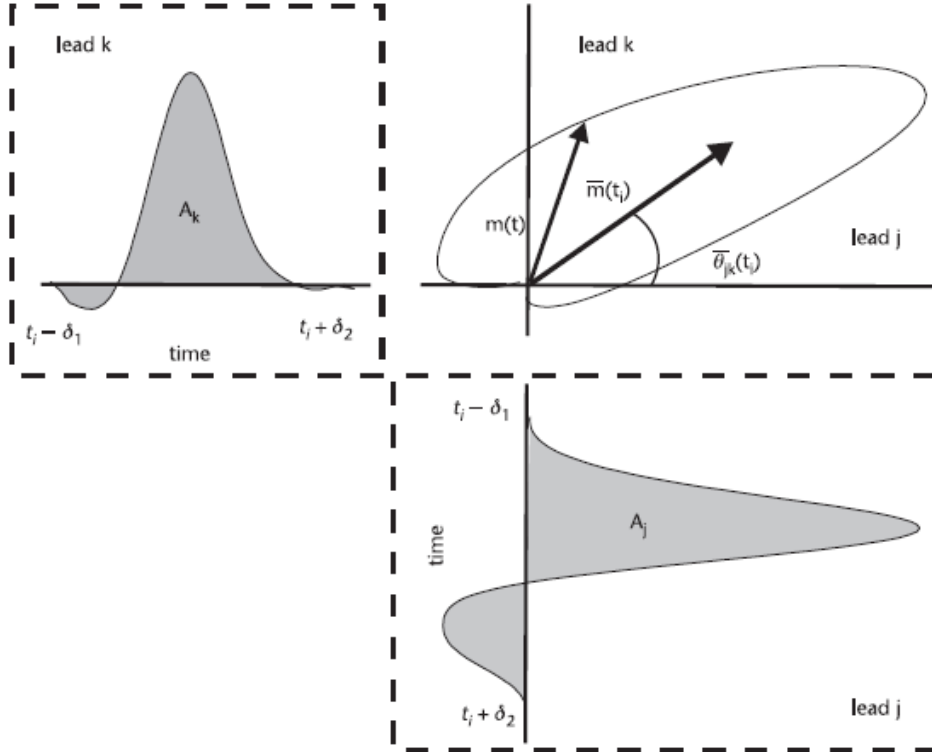


Figure 11.1: Projection of the heart's mean electrical axis on the jk -plane [7].

This EDR algorithm was chosen because it is one of the widest known methods, the method comply with the requirements of this project and a multi lead approach

might prove more robust than single lead algorithms.

The integration boundaries δ_1 and δ_2 , might be fixed or variable. A previous study have shown, that variable boundaries defined as the Q and S waves of the QRS complex, faired better than fixed boundaries (0.522 compared to 0.468) [8]. This approach is therefor adopted in this evaluation.

Lead I and II, while not strictly orthogonal, are the most common selection of leads for this method. In addition Lead I and Lead II are readily available in most ECG set ups and seem to respond well to inter-thoracic volume changes (see the pilot study in Appendix B). On this basis Lead I and Lead II are chosen in this evaluation.

11.2 Single Lead Methods Based on R-wave Amplitude or QRS Area

These methods single lead methods. In this evaluation, the choise of leads is based on the pilotstudy in Appendix B. The leads most affected by the presence or air in the lungs are Lead II and Lead V4, which are chosen for this evaluation for all single lead methods.

11.2.1 EDR2A & EDR2B: R Wave Amplitude with Respect to Baseline

Amplitude modulations of the ECG has been used to derive the respiratory signal when only single-lead ECGs are available. Typically, the amplitude of the R-wave is measured with respect to the baseline. This is a simple and widely used method, and the amplitude of the R wave is readily available in many applications.

11.2.2 EDR3A & EDR3B: R Wave Amplitude with Respect to S Wave

Studies have shown, that the EDR signal based on the measure of the R-wave amplitude with respect to the S wave amplitude obtained higher sensitivity and positive predictivity compared to the EDR signal based on the R-wave with respect to baseline [38]. For this reason this method will also be evaluated.

11.2.3 EDR4A & EDR4B: QRS Area

Another single lead approach is to obtain a EDR signal by calculating the area enclosed by the baseline and the QRS complex in a certain interval. The QRS area approach is less affected by noise compared to pure amplitude EDR methods. [17]. The boundaries of the area can be either fixed or variable. In this evaluation variable boundaries corresponding to the Q- and S wave of the QRS complex are chosen.

11.3 Methods Based Wavelet Transform or Bandpass Filtering

11.3.1 EDR5: Wavelet Transform

A different approach to EDR is to bandpass filter the single-lead ECG with a frequency band corresponding to that of the respiratory frequency. The discrete wavelet transform has been applied to the single-lead ECG and the scale corresponding to the frequency band 0.2 to 0.4 Hz can be selected as an EDR signal [50].

The Fourier transform provide information about which frequency components are contained in a given signal. It does not, however, provide information about when those frequency components are present in time. This is overcome with the wavelet transform. The wavelet transform decomposes the signal two subsignals, namely an approximation signal and a detailsignal. The upper half of the frequency components, that is from half the Nyquist-frequency, F_n , to $F_n/2$, is contained in the detail signal, while the approximation signal contain the lower half of the frequencies. This decomposition can be repeated on the approximation signal, to produce the second level of the decomposition. The process can be repeated until the approximation signal consist of only one sample. [50].

The respiratory surrogate is produced by reconstructing the detail signal at a proper level. The ECG in this thesis is sampled at 500Hz, which means that a level 10 decomposition would produce a detail signal in the frequency range of 0.24Hz to 0.49Hz which is acceptable in the context of respiration.

During the implementation of the wavelet decomposition based methods it was apparent that the method did not produce respiratory wave forms that would enable the detection of specific breaths. Several wavelets have been tried all with the same result. In Figure 11.2 the waveform produced by this method is compared to the reference waveform and the waveform produced by another EDR method.

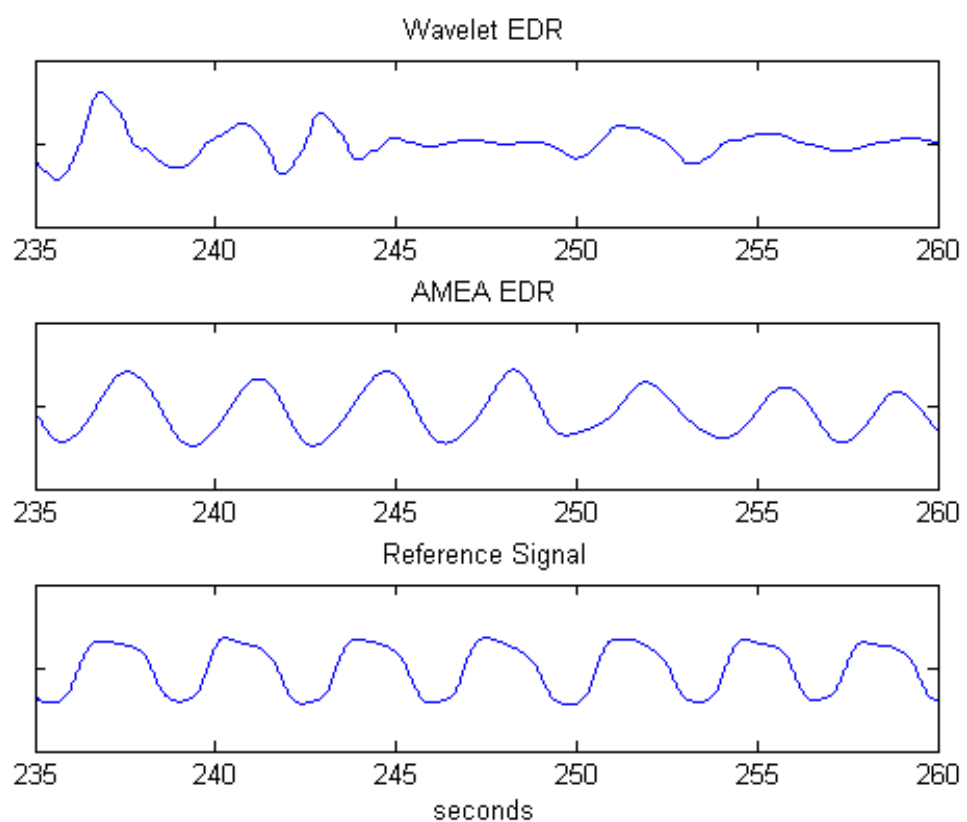


Figure 11.2: The top trace show the output of a Wavelet EDR. The middle trace is the output from an AMEA EDR and the bottom output is the trace of the reference signal.

Chapter 12

Evaluation

This chapter will describe the various stages of the evaluation of the EDR algorithms.

12.1 Reference Signal

When evaluating surrogate respiratory waveforms derived fromm the ECG, it is necessary to have a true respiratory signal, recorded simulanenous with the ECG. Various approaches exist for monitoring respiration. Generally they can be divided into two catagories; direct and indirect methods. [17]. In direct methods a sensor is connected to the airways where the flow, pressure, temperature or chemical composition of the air is measured as it passes into and out of the lungs.

Indirect methods the body volume or the movement of the thorax is recorded. Transthoracic impedance and inductance plethysmography are the indirect methods most commonly employed. In inductance plethysmography, compliant inductance loops are placed around the chest and abdomen. During inspiration and expiration the volumes of the thorax change, and this changes the area of the coils and thereby their inductance. [11,17] Direct measurements can interfere with normal respiration, but are generally more accurate. Indirect measurements can be highly accurate and does not interfere with respiration. [38]

The method available in this project is an thermistor based air flow meter. The reference signal was recorded simulatanously with a 12 lead ECG signal on four subjects as a part of this thesis. The data collection protocol can be seen in Appendix A. In compliance with the requirements, the recordings were of five minute duration. Recordings were performed on the subjects while the were lying supine on an examination bench and while they were sitting. However, only the recordings from the supine position is used in this evaluation. One of the subject were excluded from the evaluation due to a very noisy ECG recording.

12.2 Respiratory Period Estimation

The output of the EDR algorithms is a series of points, one point for each QRS complex. In order to produce af smooth respiratory surrogate, the points are in-

terpolated. This is done with cubic spline interpolation in MatLab. Now the mean of the EDR signal is subtracted from the signal. This is done in order to be able to use zero crossings as a salient point in the detection of individual breaths. The reference signal is also mean-substracted for the same reason. Individual breaths can now be detected as zero crossings in the positive direction.

The detected breaths are now manually controlled. If a breath is only detected in one of the signals, the breath is excluded in both signals. The number of excluded breaths are mentioned in the results. Often it is necessary to exclude a breath in either end of the recording. This is the case when the recording end just after the occurence of a breath in one signal and just prior to the occurence of a breath in the other signal. These exclusions of end breaths are not mentioned in the results.

When the occurence of all the breaths are detected, the duration of each breath is calculated in both signals, and the further evaluation is performed

12.3 Performance Measures

in the evaluation of the EDR methods, it is critical to have performance measures that can be compared between the EDr methods. Previous works, that has attempted to derive a respiratory signal from the ECG, have relied on visual comparsism between the EDR signal and a reference signal. Visual assesment is inherently subjective and not comparable. This section introduces the performance measures to be used in this evaluation.

12.3.1 Mean Square Error

The mean squared error of an estimate is way to quantify the difference between the values of the estimate and the true values. Mean square error measure the mean of the squares of the "errors". The error is difference between the estimate and the true value.

If Y is a series of n true values, and \hat{Y} is a series of estimates, then the mean square error (MSE) of the estimate is:

$$MSE = \frac{1}{n} \sum_{i=1}^n (\hat{Y}_i - Y_i)^2 \quad (12.1)$$

The results are presented as the root square mean error (RMSE). Which square root of the MSE.

$$RMSE = \sqrt{MSE} \quad (12.2)$$

12.3.2 Correlation Coefficient

The linear association between two variables can be expressed by Pearson's product-moment correlation coefficient, also known as Pearson's r . Pearson's r measures the correlation between two samples, X and Y , (in this case the respiratory periods from the EDR signal and from the reference air flow signal) giving a coefficient from -1 (perfect negative correlation) through 0 (no correlation) to +1 (perfect positive

correlation).

Pearson's r is defined as the covariance of the two variables divided by the product of their standard deviations [51]:

$$r = \frac{\sum_{i=1}^n (X_i - \bar{X})(Y_i - \bar{Y})}{\sqrt{\sum_{i=1}^n (X_i - \bar{X})^2 \sum_{i=1}^n (Y_i - \bar{Y})^2}} \quad (12.3)$$

In this thesis the correlation coefficient will be used to investigate the association between the series of respiratory periods derived from the reference respiratory signal and the ECG derived respiratory surrogate.

The significance of the correlations is also tested.

12.3.3 Scatter Plots

Scatterplots are used in the results to visualise the correlation. Different markers are used for different subjects. In the scatter plot a linear regression line is plotted for each subject and for the total population, while the corresponding coefficient of determination, R^2 , is noted in the legend of each scatterplot.

Chapter 13

Results

This chapter contains the results from the evaluation of the EDR methods.

EDR1 Scatter Plot

As seen in Figure 13.1, the coefficient of determination for EDR1 method was 0.465.

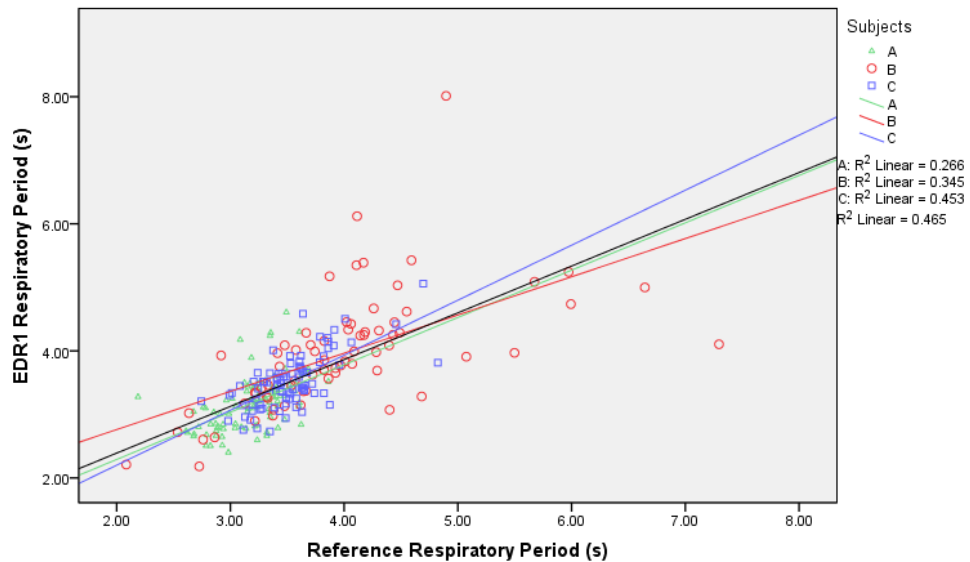


Figure 13.1: Scatterplot that visualises the correlation between the true respiratory periods and the respiratory periods derived by EDR1.

EDR2A Scatter Plot

As seen in Figure 13.2, the coefficient of determination for EDR2A method was 0.774.

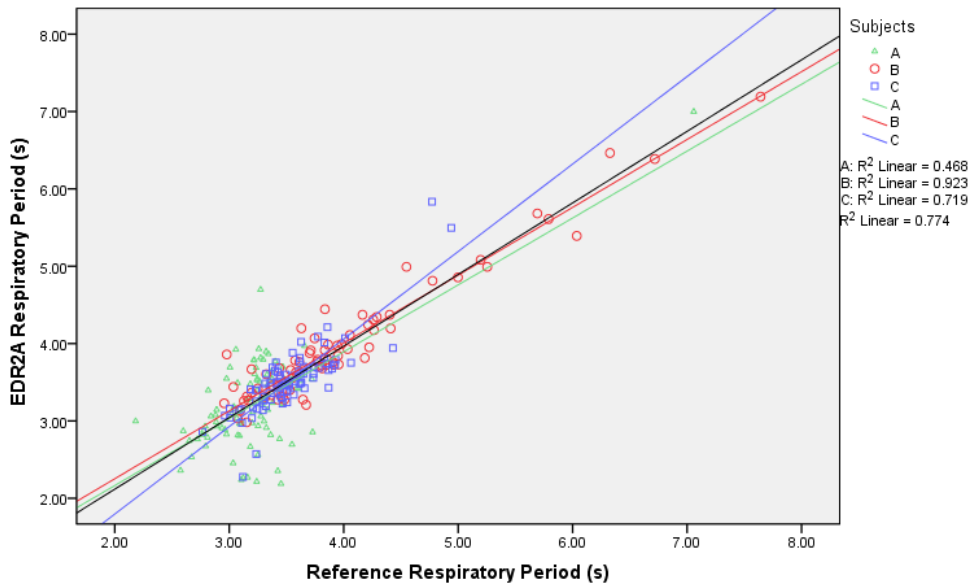


Figure 13.2: Scatterplot that visualises the correlation between the true respiratory periods and the respiratory periods derived by EDR2A.

EDR2B Scatter Plot

As seen in Figure 13.3, the coefficient of determination for EDR2B method was 0.875.

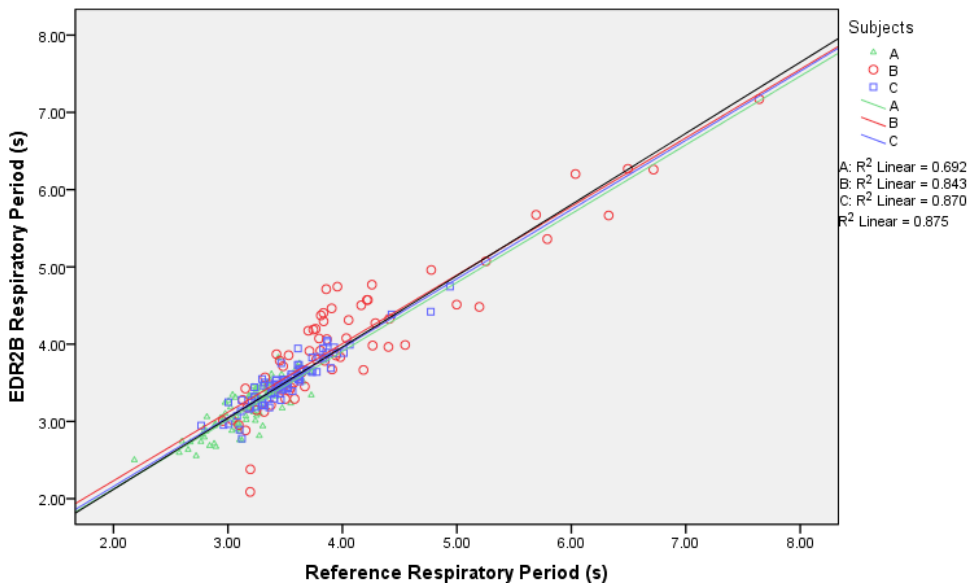


Figure 13.3: Scatterplot that visualises the correlation between the true respiratory periods and the respiratory periods derived by EDR2B.

EDR3A Scatter Plot

As seen in Figure 13.4, the coefficient of determination for EDR3A method was 0.831.

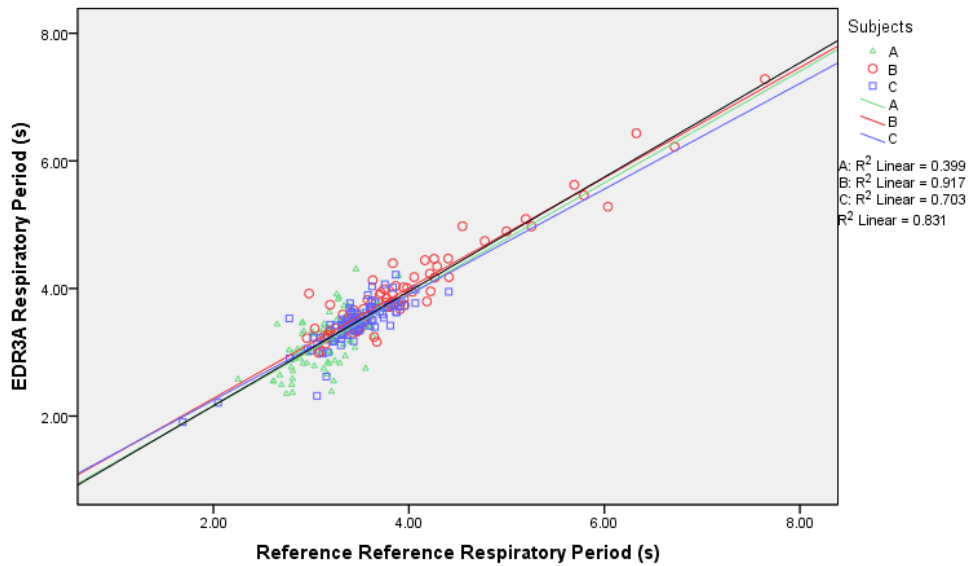


Figure 13.4: Scatterplot that visualises the correlation between the true respiratory periods and the respiratory periods derived by EDR3A.

EDR3B Scatter Plot

As seen in Figure 13.5, the coefficient of determination for EDR3B method was 0.850.

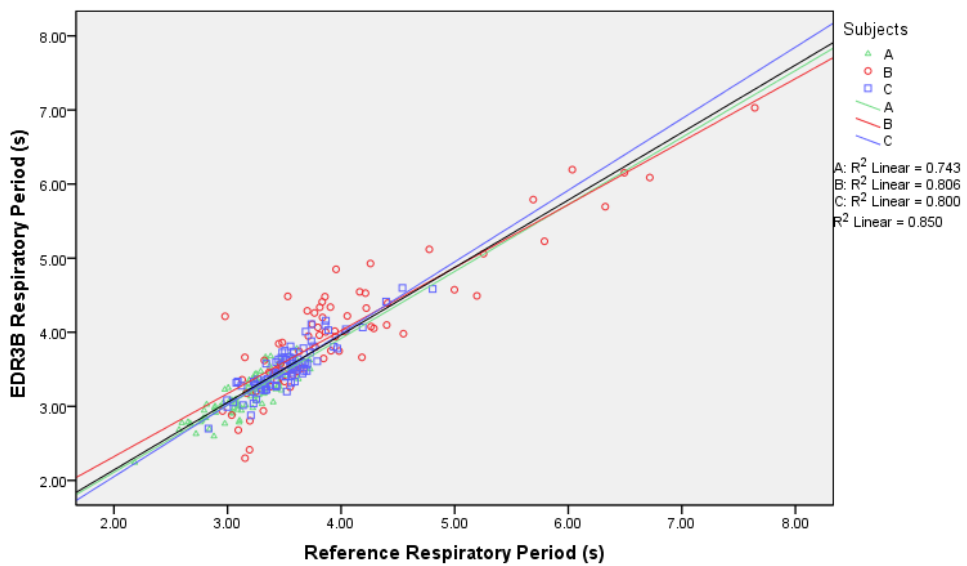


Figure 13.5: Scatterplot that visualises the correlation between the true respiratory periods and the respiratory periods derived by EDR3B.

EDR4A Scatter Plot

As seen in Figure 13.6, the coefficient of determination for EDR4A method was 0.870.

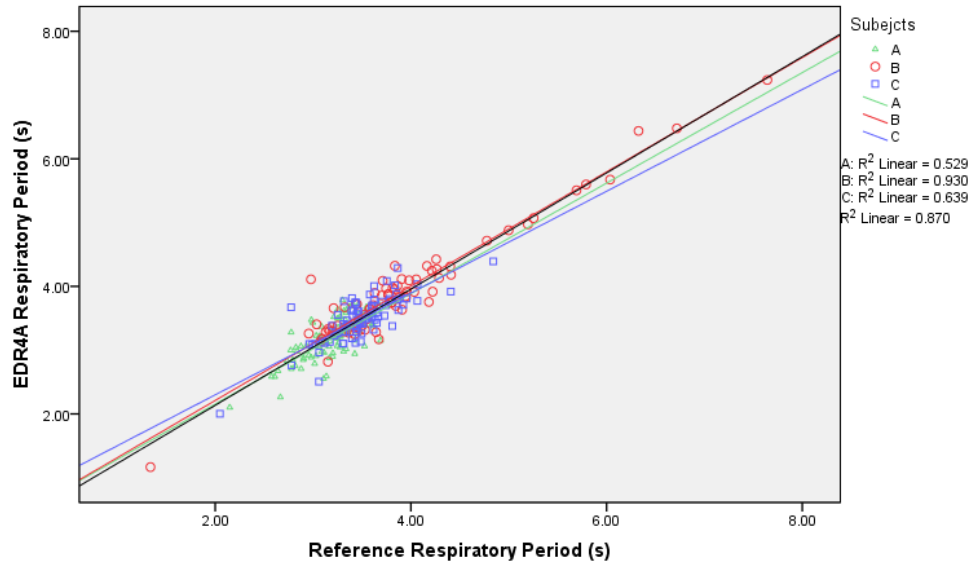


Figure 13.6: Scatterplot that visualises the correlation between the true respiratory periods and the respiratory periods derived by EDR4A.

EDR4B Scatter Plot

As seen in Figure 13.7, the coefficient of determination for EDR4B method was 0.879.

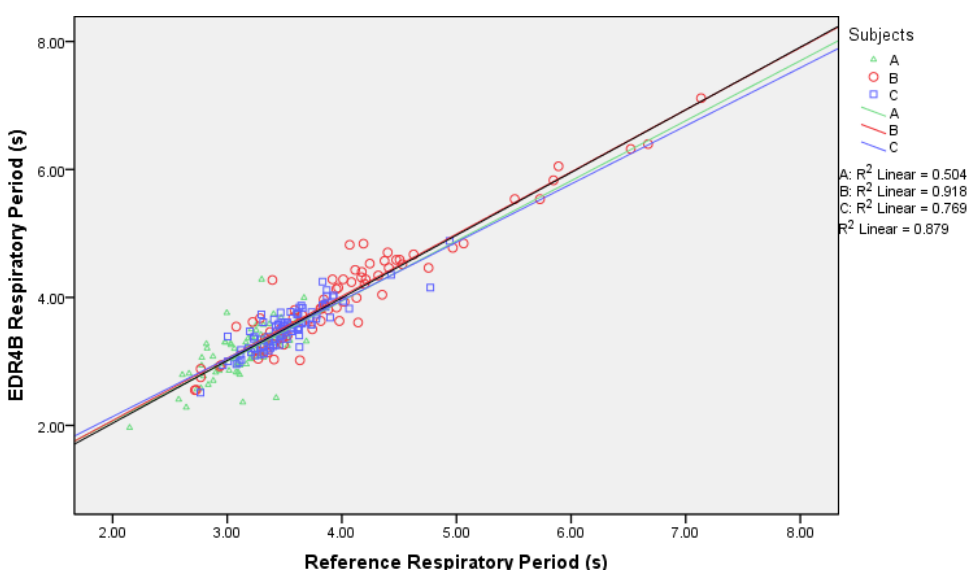


Figure 13.7: Scatterplot that visualises the correlation between the true respiratory periods and the respiratory periods derived by EDR4B.

Summary of Results

The results from the evaluation are summarised in Table 13.1. The mean respiratory duration for the reference signal is 3.190, hence the relative error ranges from 7.3% to 16.6%.

EDR Method	RMSE [s]	r	p	n	Excluded
EDR1	0.528	0.682*	0.000	250	2
EDR2A	0.339	0.880*	0.000	249	3
EDR2B	0.265	0.936*	0.000	249	2
EDR3A	0.267	0.912*	0.000	252	1
EDR3B	0.270	0.922*	0.000	250	3
EDR4A	0.233	0.933*	0.000	252	0
EDR4B	0.234	0.938*	0.000	250	3

Table 13.1: *Results from all EDR evaluations. RMS is the root mean square error of the ECG derived respiratory periods in seconds. r refers to Pearson product-moment correlation. (p) indicates the two-tailed significance of the correlation. n is the number of respiratory periods evaluated and Excluded indicates the number of respiratory periods that were excluded prior to evaluation.*

Part III

Summary

Chapter 14

Discussion

Results of the Evaluation

The aim of this thesis was to evaluate a number of EDR algorithms. The main finding of the thesis was that there was a significant correlation between the breath durations extracted from the ECG derived respiratory waveforms and the breath durations extracted from the reference signal. Surprisingly the multi lead EDR, EDR1, performed poorer with a correlation coefficient of 0.682 while the correlation coefficients of the other EDR methods are in the 0.88 to 0.94 range. This is in agreement of a study by O'Brien et al. were an identical multi lead method is compared to a method very similar to EDR2A/B. In the study by O'Brien et al. the EECG derived signals of are compared directly to af reference signal, yielding a correlation coefficient of 0.63 for the multi lead EDR and 0.78 for the single lead.

Among the EDR methods were different ECG leads were evaluated it seem that the only considerable difference is in EDR2A/B, were lead V4 out perform lead II. In all other cases, the performance of the two leads similar, although with a trend going towards lead V4.

Although not analyzed there appears to be a relatively large inter subject variability in the results, at least for the single lead EDR methods (EDR2A/B through EDR4A/B). The coefficients of determination indicate that the results of subject B is more highly correlated to the reference. It is also apparent, that the variability of the breath durations of Subject B is higher than Subject A and Subject C, who are more clustered.

EDR based on Wavelet Decomposition

One of the EDR methods, namely the one based on the concept of wavelet decomposition, proved unsuitable to be evaluated in the context of this thesis. This disagrees with the findings of other studies. Yi and Park used wavelet decomposition to derive af respiratory signal in which breath durations were identified in a manner similar to the one described in this thesis. The correlation between the series of breath durations extracted from the ECG derived signal and a reference signal was above 0.9 [50].

In the case of Yi and Park the ECG signal was sampled at $200Hz$ and the resulting EDR signal was the reconstruction of the 9th decomposition. This results in frequency range of $0.2Hz$ and $0.4Hz$. The wavelet decomposition implemented in this thesis reconstructs the signal components from the frequency range from $0.24Hz$ and $0.49Hz$, which does not entirely include the normal respiratory frequency range, which lie between $0.2Hz$ and $0.33Hz$.

Reference Signal

The reference signal chosen in the evaluation was a respiratory airflow signal. The air flow meter measures the exchange of air in the lungs, while the EDR methods are more likely to measure the state of which the thorax is in at any given time. This can be corrected for by integrating the air flow signal. However, one have to take great care in doing so, as even a small error in the measurement will accumulate, causing a drift in the signal.

Another challenge with the choice of the airflow meter is that it obstructs the airways, and thus inhibits normal spontaneous breathing. Considering these challenges, indirect respiration measurements might be preferable in future studies.

Performance Measures

This thesis applies two performance measures; the root mean square error (RMSE) to investigate the error between the true breath duration and the estimate, and Pearson's Product-Moment Correlation to investigate for correlation. Both performance measures have been widely used in the context of EDR studies [14, 21, 28]

Chapter 15

Conclusion

In this thesis a literature review of the concept ECG derived respiration was conducted. Five of the EDR methods were selected for implementation. One of the methods required two ECG leads, while the other four were single lead methods. Four of the EDR methods required preprocessing of the ECG. The preprocessing consisted of filtering stage, in which the ECG was denoised and the respiratory information was enhanced. The preprocessing also included the detection of the QRS complexes of the ECG.

In order to evaluate and compare the performance of the EDR methods, a 12-lead ECG and a respiratory air flow signal were recorded simultaneously. The signal recordings were of five minute duration and were conducted on four healthy male subjects. The subjects lay supine for the duration of the recording and were asked to breath spontaneously. The recordings of one of the subjects were excluded from the evaluation, due to a noisy ECG recording.

One of the implemented EDR methods is based on the partial reconstruction of wavelet decomposition, the output of which is a smooth waveform. However, this EDR method did not produce feasible waveforms, when directly compared to the reference airflow signal. It was therefore excluded from the evaluation. The output of the remaining EDR algorithms is a series of points, which were interpolated to create a surrogate respiratory waveform.

In both the surrogate respiratory signals and in the reference respiratory signal, salient points were detected in order to identify individual breaths. The performance of the EDR methods were now evaluated by comparing the duration of the individual breaths identified in the derived signals with the duration of the corresponding breaths identified in the reference signal. For the evaluation two performance measures were chosen, namely RMSE and correlation in the form of Pearson's r.

With the exception of the wavelet transform based EDR, all the methods fared well. Correlation coefficients ranged from 0.682 to 0.938 and all correlations were significant. The RMSE ranged from 0.233 seconds to 0.528 seconds.

Bibliography

- [1] *SEER 12, 12-Channel Holter ECG Digital Recorder, User Manual.* GE Health-care, 2049152-010 revision a edition, 2010.
- [2] About google scholar. <http://scholar.google.dk/intl/en/scholar/about.html>, Visited August 31st 2013.
- [3] Intrinsic conduction system of the heart. <http://europace.oxfordjournals.org/content/9/12/1163/F1.large.jpg>, Visited May 20th 2013.
- [4] Matlab - the language of technical computing. <http://www.mathworks.se/products/matlab/>, Visited August 31st 2013.
- [5] Pubmed. <http://www.ncbi.nlm.nih.gov/pubmed>, Visited August 31st 2013.
- [6] Shivaram P. Arunachalam and Lewis F. Brown. Real-time estimation of the ecg-derived respiration (edr) signal using a new algorithm for baseline wander noise removal. *31st Annual International Conference of the IEEE EMBS Minneapolis, Minnesota, USA*, pages 5681–5684, September 2009.
- [7] Raquel Bailón, Leif Sörnmo, and Pablo Laguna. Chapter 8 - ecg-derived respiratory frequency estimation. In Gari D. Clifford, Francisco Azuaje, and Patrick E. McSharry, editors, *Advanced Methods and Tools for ECG Data Analysis*. Artech House, Inc, 2006. ISBN -10: 1-58053-966-1.
- [8] David Caggiano and Stanley Reisman. Respiration derived from the electrocardiogram: A quantitative comparison of three different methods. *Proceedings of IEEE 22nd Annual NE Bioengineering Conference*, pages 103–104, 1996.
- [9] Philip de Chazal et al. Automated processing of the single-lead electrocardiogram for the detection of obstructive sleep apnoea. *IEEE Transactions on Biomedical Engineering*, 50(6):686–696, June 2003.
- [10] A. Despopulos and S. Silbernagl. *Color Atlas of Physiology*. Number ISBN 3-13-545005-8. Thieme, 5th edition edition, 1998.
- [11] Dobromir Dobrev and Ivan Daskalov. Two-electrode telemetric instrument for infant heart rate and apnea monitoring. *Medical Engineering and Physics*, 20: 729–734, 1998.
- [12] G. Dower. On deriving the electrocardiogram from vectorcardiographic leads. *Clinical Cardiology*, 3:87–95, 1980.

BIBLIOGRAPHY

- [13] A. L. Goldberger et al. Physiobank, physiotoolkit, and physionet: Components of a new research resource for complex physiologic signals. *Circulation*, 101(23):e215–e220, June 2000.
- [14] Christina Orphanidou et al. Spectral fusion for estimating respiratory rate from the ecg. *Proceedings of the 9th International Conference of Information Technology and Applications in Biomedicine, Larnaca, Cyprus*, November 2009.
- [15] Dirk Cysarz et al. Comparison of respiratory rates derived from heart rate variability. *Annals of Biomedical Engineering*, 36(12):2085–2094, 2008.
- [16] G. Hahn et al. Changes in the thoracic impedance distribution under different ventilatory conditions. *Physiological Measurement*, 16:A161–A173, August 1995.
- [17] George B. Moody et al. Derivation of respiratory signals from multilead ecgs. *Computers in Cardiology*, 12:113–116, 1985.
- [18] G.M. Friesen et al. A comparison of the noise sensitivity of nine qrs detection algorithms. *IEEE Transactions on Biomedical Engineering*, (1):85–98, january 1990.
- [19] Homer Nazeran et al. Reconstruction of respiratory patterns from electrocardiographic signals. *2nd International Conference on Bioelectromagnetism, Melbourne, Australia*, pages 183–184, February 1998.
- [20] J. Mateo et al. Analysis of heart rate variability in the presence of ectopic beats using the heart timing signal. *IEEE Transactions on Biomedical Engineering*, 50:334–343, 2003.
- [21] Justin Boyle et al. Automatic detection of respiratory rate from ambulatory single-lead ecg. *IEEE Transactions on Information Technology in Biomedicine*, 13(6):890–896, November 2009.
- [22] K. Behbehani et al. An investigation of the mean electrical axis angle and respiration during sleep. *Proceedings of the Second Joint EMBS/BMES Conference, Houston, TX, USA*, pages 1550–1551, October 2002.
- [23] L. Zhao et al. Derivation of respiration from electrocardiogram during heart rate variability studies. *IEEE Computers in Cardiology*, 21:53–56, 1994.
- [24] Leonard S. Dreifus et al. Heart rate variability for risk stratification of life-threatening arrhythmias. *Journal of the American College of Cardiology*, 22(3):948–950, September 1993.
- [25] Lorena S. Correra et al. Performance evaluation of three methods for respiratory signal estimation from the electrocardiogram. *30th Annual International IEEE EMBS Conference, Vancouver, British Columbia, Canada*, (6):4760–4763, August 2008.
- [26] M. Vararini et al. Adaptive filtering of ecg signal for deriving respiratory activity. *Proceedings of Computers in Cardiology, IEEE Computer Society Press*, 59:621–624, 1990.
- [27] P.D. Larsen et al. Respiratory sinus arrhythmia in conscious humans during spontaneous respiration. *Respiratory Physiology and Neurobiology*, (174):111–118, April 2010.

BIBLIOGRAPHY

- [28] Philip Langley et al. A robust method for ecg-based estimation of the respiratory frequency during stress testing. *IEEE Transactions of Biomedical Engineering*, 57(4):821–829, April 2010.
- [29] Ramon Pallas-Areny et al. The effects of respiration-induced heart movements on the ecg. *IEEE Transactions on Biomedical Engineering*, 36(6):585–590, June 1989.
- [30] S. Leanderson et al. Estimation of the respiratory frequency using spatial information in the vcg. *Medical Engineering and Physics*, 25:501–507, 2003.
- [31] Jacques felblinger and Chris Boesch. Amplitude demodulation of the electrocardiogram signal (ecg) for respiration monitoring and compensation during mr examinations. *Magnetic Resonance in Medicine*, 38(1):129–136, July 1997.
- [32] Patrick S. Hamilton and Willis J. Tompkins. Quantitative investigation of qrs detection rules using the mit/bih arrhythmia database. *IEEE Transactions on Biomedical Engineering*, BME-33(12):1157–1165, December 1986.
- [33] I. Kestin. Control of heart rate. *Update in Anaesthesia*, (3):15–16, 1993.
- [34] Ziad Bou Khaled and Gilbert Farges. First approach for respiratory monitoring by amplitude demodulation of the electrocardiogram. *Engineering in Medicine and Biology Society, 1992 14th Annual International Conference of the IEEE*, 6:2535–2536, 1992.
- [35] Raquel l Bailón et al. A robust method for ecg-based estimation of the respiratory frequency during stress testing. *IEEE Transactions of Biomedical Engineering*, 53(7):1273–1285, July 2006.
- [36] Jaakko Malmivuo and Robert Plonsey. *Bioelectromagnetism - Principles and Applications of Bioelectric and Biomagnetic Fields*. Number ISBN-13: 978-0195058239. Oxford University Press, 1995.
- [37] F.H. Martini. *Fundamentals of Anatomy and Physiology*. Number ISBN: 0-321-31198-1. Pearson, 7th edition edition, 2006.
- [38] C. L. Mason and L. Tarassenko. Quantitative assesment of respiratory derivation algorithms. *Proceedings of the 23rd Annual EMBS International Conference*, pages 1998–2001, October 2001.
- [39] Nobelprize.org. The electrocardiogram - looking at the heart of electricity. <http://www.nobelprize.org/educational/medicine/ecg/ecg-readmore.html>, Visited May 20th 2013.
- [40] Ciara O'Brien and Conor Heneghan. A comparison of algorithms for estimation of a respiratory signal from the surface electrocardiogram. *Computers in Biology and Medicine*, 37:305–314, 2007.
- [41] Task Force of The European Society of Cardiology, The North American Society of Pacing, and Electrophysiology. Heart rate variability - standards of measurement, physiological interpretation, and clinical use. *European Heart Journal*, 17:354–381, 1996.
- [42] Sung-Bin park et al. An improved algorithm for respiration singal extraction from electrocardiogram measured by conductive tectile electrodes using instantaneous frequency estimation. *Medical and Biological Engineering and Computing*, 46:147–158, 2008.

BIBLIOGRAPHY

- [43] D. C. Randall and Y. M. El-Wazir. *ECG Interpretation*. Number ISBN 1593771800. Hayes Barton Press, 2004.
- [44] Leif Sörnmo. Vector cardiographic loop alignment and morphologic beat-to-beat variability. *IEEE Transactions on Biomedical Engineering*, 45(12):1401–1413, December 1998.
- [45] Juan Sztajsel. Heart rate variability: a noninvasive electrocardiographic method to measure autonomic nervous system. *Swiss Medical Weekly*, (134):514–522, September 2004.
- [46] C.M.A. van Ravenswaaij-Arts et al. Heart rate variability. *Annals of Internal Medicine*, 118(6):436–447, March 1993.
- [47] Robert C. Wang and Thomas W. Calvert. A model to estimate respiration from vectorcardiogram measurements. *Annals of Biomedical Engineering*, 2:47–57, 1974.
- [48] John G. Webster. *Medical Instrumentation - Application and Design*. Number ISBN 0-471-15368-0. Wiley, 3rd edition edition, 1998.
- [49] Baxter F. Womack. The analysis of respiratory sinus arrhythmia using spectral analysis and digital filtering. *IEEE Transactions on Biomedical Engineering*, BME-18(6):399–409, November 1971.
- [50] W.J. Yi and K. S. Park. Derivation of respiration from ecg measured without subject's awareness using wavelet transform. *Proceedings of the Second Joint EMBS/BMES Conference, Houston, TX, USA*, pages 130–131, October 2002.
- [51] Jerrold H. Zar. *Biostatistical Analysis*. Number ISBN-13: 978-0-13-206502-3. Pearson, 5th edition edition, 2010.

Part IV

Appendix

Appendix A

Data Collection Protocol

The signals for the evaluation of the EDR algorithms were recorded in the C laboratory at the Department of Health Science and Technology at Aalborg University. This protocol describes the procedure for the data collection.

Objective

The objective of this protocol is to simultaneous record an ECG signal and a respiratory flow signal in a number of subjects.

Instruments and Materials

- General Electrics SEER 12. A 12 channel digital holter ECG Recorder.
- Disposable ECG electrodes.
- Sensiron SFM 3000 Mass Flowmeter. A thermistor based flow meter.
- Laptop installed with Evaluation Kit EK-F3X data acquisition software.
- Inflatable face mask and HME filter.
- Examination bed.
- Metronome app on smartphone.
- Stop watch.

Subjects

The data acquissition was conducted on four male volunteers. The age of the subjects ranged from 28 to 42. All subjects were considered normal, that is, they were not known to suffer from any cardiac, or respiratory disorders, etc.

ECG

The ECG electrodes were placed in the standard 12-lead configuration. The ECG signal was obtained at $128Hz$ and resampled to $500Hz$.

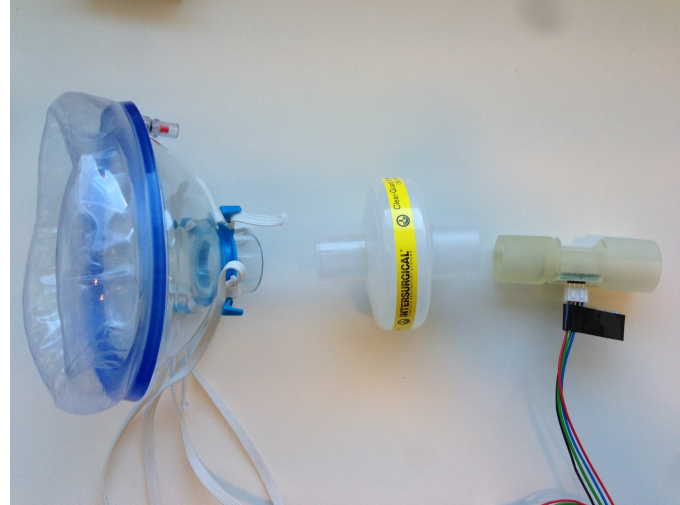


Figure A.1: *From left to right: The face mask, the HME filter, and the flow meter.*

Airflow

The flowmeter was connected to the HME filter which in turn is connected to the face mask (See figure A.1). Using elastic straps, the face mask was strapped to the face of the subject (See figure A.2). The subject was able to breath freely from both the nose and the mouth, while there was an airtight seal between the face of the subject and the mask. The airflow signal was sampled at $128Hz$.



Figure A.2: *The face mask, filter, and flowmeter strapped to the face of a subject.*

Procedure

For each subject the procedure was as follows:

- The face mask was cleaned with alcohol.
- The ECG electrodes were placed on the subject and the ECG recording was initiated.
- The face mask and EMH filter was strapped to the face of the subject.
- The subject was asked to lie in a supine position on the examination bed.
- The flowmeter recording was initiated.
- The flowmeter was tapped five times in rapid succession on the V2 electrode. This induced simultaneous fiducial points in both the ECG signal and the flow signal, to be used later for synchronisation.
- The flowmeter was placed in the facemask of the subject, who was asked to breath normally for a 6 minute epoch, ensuring at least 5 minutes of undisturbed recording.
- After the 6 minute epoch, the subject was asked to sit on the edge of the examination bed, while breathing normally for another 6 minute epoch.
- After the sitting epoch, the flow meter was removed from the face mask.
- The flowmeter was again tapped 5 in rapid succession on the V2 electrode, inducing another set of fiducial points in both signals, indicating that the recording has ended.
- Both recordings (ECG and flow) were stopped and stored.

Additional Data

In addition to the protocol, one of the subjects performed a more elaborate respiratory regime. A number of different respiratory frequencies and depths were performed. The regime was as follows:

- 120 seconds of paced respiration (paced to 12 breaths per minute).
- 30 seconds of breath hold after normal inspiration.
- 120 seconds of paced respiration (paced to 20 breaths per minute).
- 30 seconds of breath hold after normal expiration.
- 120 seconds of deep/heavy respiration.
- 30 seconds of breath hold after deep inspiration.
- 120 seconds of shallow respiration.
- 30 seconds of breath hold after full expiration.

The subject was asked to breath at a paced rate of 12 and 20 breaths per minute ($0.2Hz$ and $0.33Hz$ respectively), which forms the extremes of normal resting respiration in adults (See D). The breathing rate of the subject was paced using a metronome application on a smartphone, with a visual pendulum-swing. The subject was asked to match his inspiration and expiration to the rate at which the pendulum swung. For example, when the pendulum swung to the right, the subject was asked to pace himself so that his inspiration would be of the same duration as the right swing. s

Appendix B

Pilot Study

Objective

The objective of this pilot experiment is to determine how the different ECG leads are affected by the amount of air the lungs are filled with.

Procedure

As described in the data collection protocol, see Appendix A, one subject performed a series of breath holds. Four breath holds was performed under four different conditions:

- Breath hold after normal inspiration.
- Breath hold after normal expiration.
- Breath hold after deep inspiration.
- Breath hold after full expiration.

All breath hold epochs endures for 30 seconds. During the breath holds the 12 lead ECG was collected. The ECG was filtered with the pre processing procedure described in section 10.1. The maximum QRS amplitude of each ECG signal was chosen as the comparison measure.

Results

Comparison of Breath Hold after Normal Inspiration and after Normal Expiration

Table B.1 show the maximum QRS amplitudes of each ECG lead during breath hold after normal inspiration and after normal expiration, and the absolute and relative difference between the two conditions.

Lead	$V_{Expired} [\mu V]$	$V_{Inspired} [\mu V]$	$difference [\mu V] ([\%])$
LeadI	764	651	-113 (-15)
LeadII	1454	1776	322 (22)
V1	1935	1840	-95 (-5)
V2	2737	2211	-526 (-19)
V3	1501	1563	62 (4)
V4	1835	2249	414 (23)
V5	2348	2644	296 (13)
V6	2425	2391	-34 (-1)

Table B.1: *Maximum QRS amplitudes of each ECG lead during breath hold after normal inspiration and after normal expiration, and the absolute and relative difference between the two conditions.*

Figure B.1 show a section of the ECG signal for each lead during breath hold after normal expiration (red trace) and after normal inspiration (blue trace).

Comparison of Breath Hold after Deep Inspiration and after Full Expiration

Table B.2 show the maximum QRS amplitudes of each ECG lead during breath hold after deep inspiration and after full expiration, and the absolute and relative difference between the two conditions.

Lead	$V_{Expired} [\mu V]$	$V_{Inspired} [\mu V]$	$difference [\mu V] ([\%])$
LeadI	1133	406	-727 (-64)
LeadII	1356	1753	397 (29)
V1	1999	1547	-452 (-22)
V2	2854	1734	-1120 (-39)
V3	1464	1473	9 (1)
V4	1634	2072	438 (26)
V5	2050	2084	34 (2)
V6	2067	1630	-437 (-21)

Table B.2: *Maximum QRS amplitudes of each ECG lead during breath hold after deep inspiration and after full expiration, and the absolute and relative difference between the two conditions.*

Figure B.2 show a section of the ECG signal for each lead during breath hold after deep expiration (red trace) and after full inspiration (blue trace).

APPENDIX B. PILOT STUDY

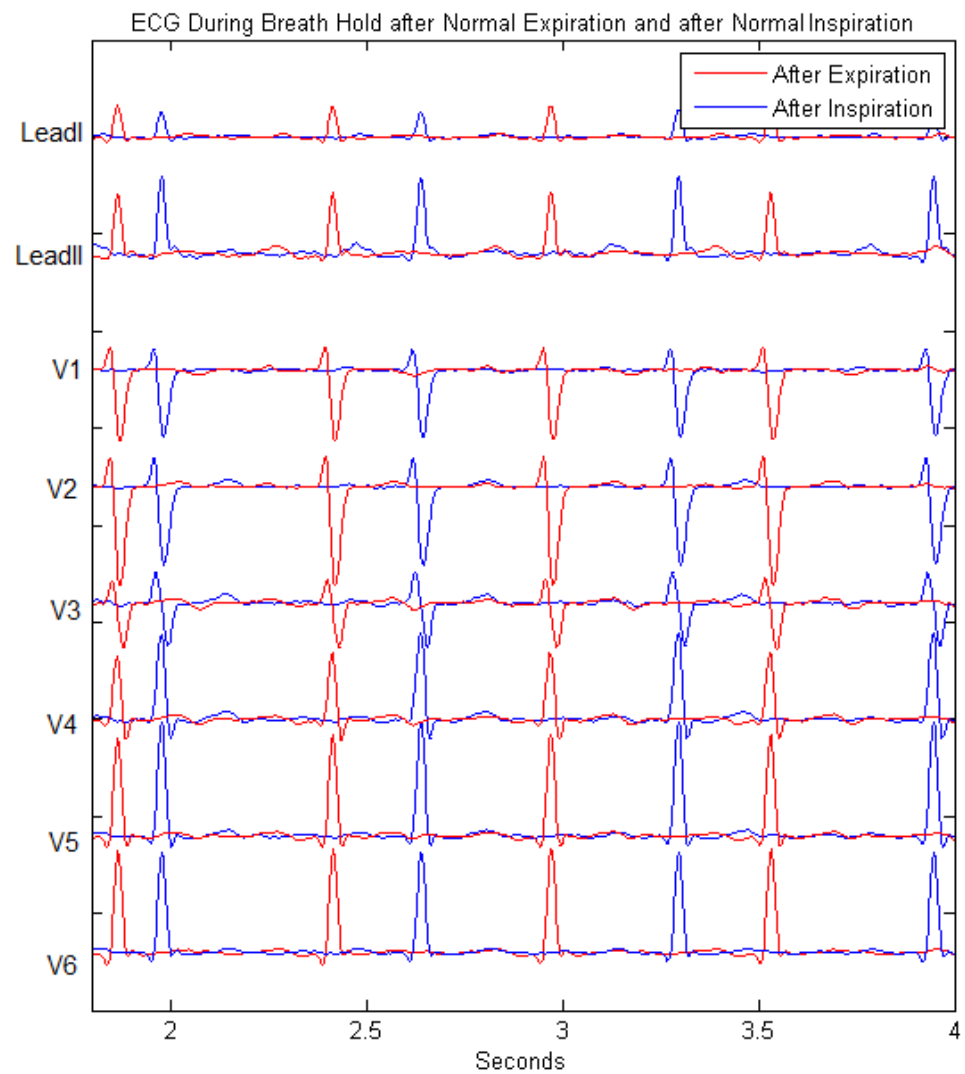


Figure B.1: *ECG signal for each lead during breath hold after normal expiration (red trace) and after normal inspiration (blue trace).*

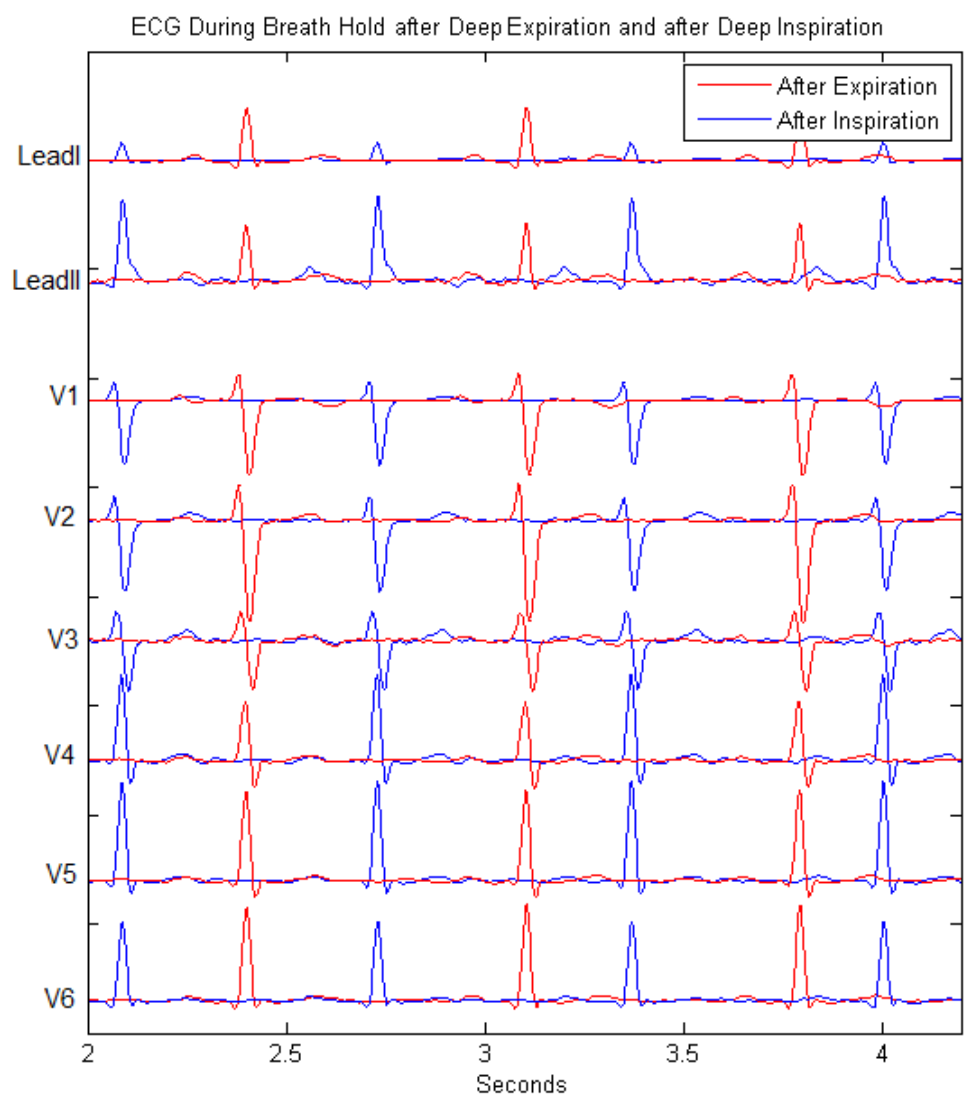


Figure B.2: *ECG signal for each lead during breath hold after deep expiration (red trace) and after full inspiration (blue trace).*

Discussion and Conclusion

Figure B.1 shows a section of ECG during breath hold after normal inspiration (red) and after normal expiration (blue). It can be seen, that most of the ECG leads are somewhat affected. In addition it can be seen, that the amplitude of the QRS complex might be attenuated or amplified depending on the ECG lead.

The same pattern, however enhanced, can be seen in Figure B.2, which show a section of ECG during breath hold after deep inspiration (red) and after normal expiration (blue).

The scope of this thesis is normal breathing. The leads most affected by normally airfilled lungs are lead II and lead V4#.

Appendix

C

Synthesis of the VCG

Several methods have been proposed for the synthesis of the VCG from the 12-lead ECG. However the inverse transformation transform of Dower is the most commonly used. In 1980 Dower et al. proposed a method for deriving the 12-lead ECG lead by lead as the weighted sum of the VCG-leads X, Y, and Z of the Frank lead VCG [12]. This transform uses coefficients based on the on the image surface data from the original torso studies by Frank.

The transformation operation to give the the leads V to V6, lead I and lead II (the eight independent ECG-leads of the 12 lead ECG) is given by: [7]

$$s(n) = Dv(n) \quad (\text{C.1})$$

where $s(n) = [V1(n) V2(n) V3(n) V4(n) V5(n) V6(n) I(n) II(n)]^T$ and $v(n) = [X(n) Y(n) Z(n)]^T$ contain the voltage level of the corresponding leads, n is the sample index, and D is the Dower tranformation matrix: [7]

$$D = \begin{bmatrix} -0.515 & 0.157 & -0.917 \\ 0.044 & 0.164 & -1.387 \\ 0.882 & 0.098 & -1.277 \\ 1.213 & 0.127 & -0.601 \\ 1.125 & 0.127 & -0.086 \\ 0.831 & 0.076 & 0.230 \\ 0.632 & -0.235 & 0.059 \\ 0.235 & 1.066 & -0.132 \end{bmatrix} \quad (\text{C.2})$$

From C.1 and C.2 it follows that the VCG leads can be synthesised from the eight independent leads of the 12-lead ECG by: [7]

$$v(n) = Ts(n) \quad (\text{C.3})$$

where $T = (D^T D)^{-1} D^T$ is the inverse Dower transformation matrix given by: [7]

$$T = \begin{bmatrix} -0.172 & -0.074 & 0.122 & 0.231 & 0.239 & 0.194 & 0.156 & -0.010 \\ 0.057 & 0.019 & -0.106 & -0.022 & 0.041 & 0.048 & -0.227 & 0.887 \\ -0.229 & -0.310 & -0.246 & -0.063 & 0.055 & 0.108 & 0.022 & 0.102 \end{bmatrix} \quad (\text{C.4})$$

Appendix D

Respiration

The aim of this appendix is to give a short introduction to the respiration system. The primary function of the respiratory system is to meet the respiratory demands of cells. That is, to deliver a steady supply of oxygen to the cells of the body and to remove the carbon dioxide released by the cells.

In this appendix, the emphasis will be on external respiration, or breathing, which is the physical movement of air into or out of the lungs. This appendix will cover the mechanics of ventilation and the different respiratory volumes and capacities. The appendix is written on the background of the following references [10, 37].

Mechanics of Ventilation

Respiration is an involuntary act controlled the autonomic nervous system via the medulla oblongata of the brain. The medulla oblongata senses blood levels of carbon dioxide and triggers respiration at increased carbon dioxide levels. To a certain degree, it is possible to temporarily voluntarily override the autonomic control of respiration.

During respiration, air is moved into and out of by changing the volume of the lungs. The volume changes in the lungs are facilitated by contractions of skeletal muscles, namely, the intercostal muscles and the diaphragm.

At inspiration the intercostal muscles and the diaphragm contract to expand the chest cavity. Specifically; the intercostal muscles move the rib cage out and upwards, while the diaphragm flattens and moves downwards. This facilitates a decrease in internal air pressure, which forces air from outside the thorax into the lungs to equalize the pressure difference.

At normal expiration, intercostal muscles and the diaphragm relax and return to their resting positions. This in turns reduce the size of the thoracic cavity, thereby increasing the pressure, forcing air out of the lungs. In normal individuals no muscle contraction involved in expiration. This process is simply driven by the elastic recoil of the lungs. However, during periods of higher metabolic rate, e.g. during exercise and during voluntary deep expiration, the abdominal and the internal intercostal

muscles assist the expiration.

Respiratory Rates, Volumes, and Capacities

The respiratory system is able to adapt to meet different levels of metabolic need by increasing or decreasing the respiratory rate and volume.

Respiratory rate is the number of breaths taken within a set amount of time, usually one minute. Normal respiratory rate, called eupnea, ranges from 12 to 20 breaths per minute in resting adults.

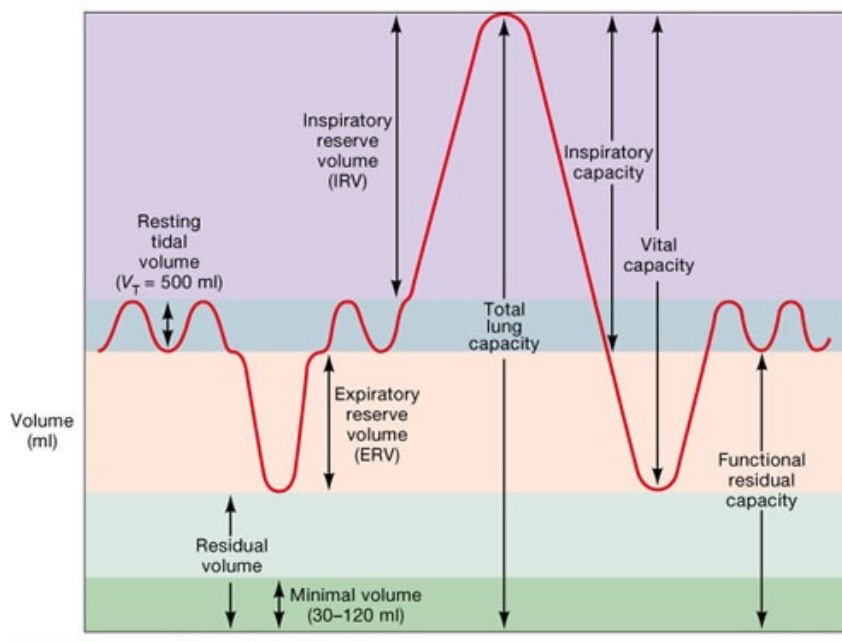


Figure D.1: *The respiratory volumes and capacities [37].*

The respiratory volumes and capacities are the amount of air inspired, expired and stored within the lungs. See figure D.1.

- **Tidal volume:** The amount of air which is shifted in the lungs during normal resting respiration. The average tidal volume is 500ml .
- **Residual volume:** The amount of air left in the lungs following a maximal expiration. The residual volume of a prevents the lungs from collapsing. The average residual volume is 1200ml .
- **Minimal volume:** Should the of the lungs fall below this volume, the lungs will collapse. The average minimal volume is $30 - 120\text{ml}$.
- **Expiratory reserve volume:** The amount of extra air expired, above tidal volume, during a forced full expiration. The average expiratory reserve volume volume is 1300ml .

-
- **Inspiratory reserve volume:** The amount of extra air inspired, above tidal volume, during a full forced inspiration. The average inspiratory reserve volume is $3000ml$.
 - **Total lung capacity:** The total volume of the lungs, including the residual volume. The average total lung capacity is $6000ml$.
 - **Inspiratory capacity:** The sum of the tidal volume and the inspiratory reserve volume. The average inspiratory capacity is $3500ml$.
 - **Vital capacity:** The total volume of usable of the lungs which is under voluntary control. The average vital capacity is $4800ml$.
 - **Functional residual capacity:** The total volume of air left in the lungs after a normal resting expiration. The average functional residual capacity is $2500ml$.

The respiratory minute volume is the volume of air inspired or expired from an individual's lungs per minute. Thus it is not volume as its name implies, but a flow. Under normal resting circumstances the respiratory minute volume equals the respiratory rate times the tidal volume. A normal minute volume during rest is about 6-10 liters per minute in adults.

Appendix E

Characteristics of QRS Detection Filters

This appendix contains the frequency and phase response of the filters of stage 1 of the QRS detector. See section 10.2.

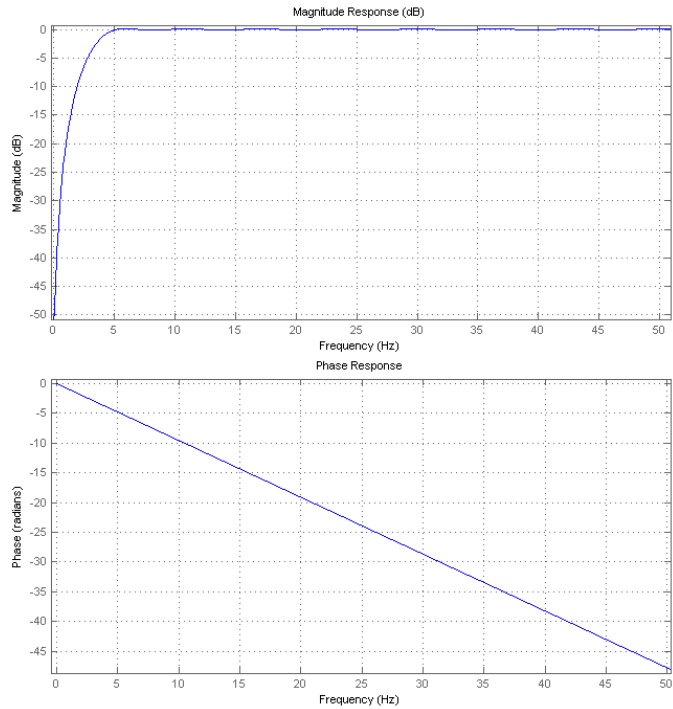


Figure E.1: *High pass filter frequency and phase response (dB/HZ and deg/Hz)*

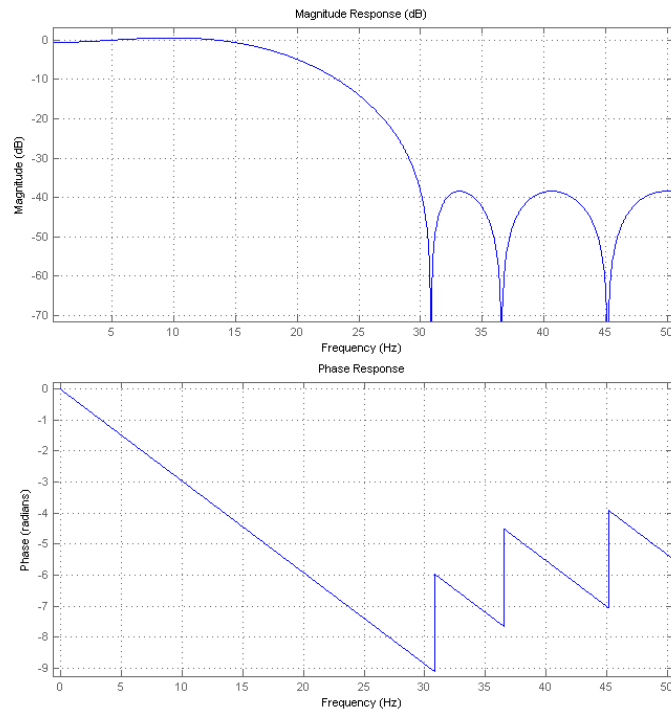


Figure E.2: Low pass filter frequency and phase response (dB/HZ and deg/Hz)